the plant journal

SEB SOCIETY FOR EXPERIMENTAL BIOLOGY

The Plant Journal (2023) doi: 10.1111/tpj.16387

SPECIAL ISSUE ARTICLE

Natural variation in *Brachypodium distachyon* responses to combined abiotic stresses

Ella Ludwig[1], Joshua Sumner[1], Jeffrey Berry[1,2], Seth Polydore[1], Tracy Ficor[1], Erica Agnew[1], Kristina Haines[1], Kathleen Greenham[1,3], Noah Fahlgren[1], Todd C. Mockler[1,†] and Malia A. Gehan[1,*]

[1]*Donald Danforth Plant Science Center, St. Louis, Missouri 63132, USA,*
[2]*Bayer Crop Sciences, St. Louis, Missouri 63017, USA, and*
[3]*University of Minnesota, St. Paul, Minnesota 55108, USA*

Received 4 March 2023; revised 26 June 2023; accepted 5 July 2023.
*For correspondence (e-mail mgehan@danforthcenter.org).
†Deceased

SUMMARY

The demand for agricultural production is becoming more challenging as climate change increases global temperature and the frequency of extreme weather events. This study examines the phenotypic variation of 149 accessions of *Brachypodium distachyon* under drought, heat, and the combination of stresses. Heat alone causes the largest amounts of tissue damage while the combination of stresses causes the largest decrease in biomass compared to other treatments. Notably, Bd21-0, the reference line for *B. distachyon*, did not have robust growth under stress conditions, especially the heat and combined drought and heat treatments. The climate of origin was significantly associated with *B. distachyon* responses to the assessed stress conditions. Additionally, a GWAS found loci associated with changes in plant height and the amount of damaged tissue under stress. Some of these SNPs were closely located to genes known to be involved in responses to abiotic stresses and point to potential causative loci in plant stress response. However, SNPs found to be significantly associated with a response to heat or drought individually are not also significantly associated with the combination of stresses. This, with the phenotypic data, suggests that the effects of these abiotic stresses are not simply additive, and the responses to the combined stresses differ from drought and heat alone.

Keywords: *Brachypodium distachyon*, bioenergy, high-throughput phenotyping, natural variation, drought, heat, abiotic stress, climate, local adaptation, genome-wide association, GWAS.

INTRODUCTION

The increasing global population is likely to create several challenges in the coming decades. The world population is expected to reach 9.8 billion people by the year 2050, which means there will be nearly 2 billion additional people on the planet to feed in fewer than 30 years (United Nations, 2019). With more than a billion people in the world already experiencing some form of food insecurity, the increasing global population creates an even higher demand for food, fuel, and fiber, that current production levels cannot meet (Conway, 2012; FAO, IFAD, UNICEF and WHO, 2020; Roy et al., 2006; Swaminathan, 2012).

An additional complication is that future crops will need to withstand the changing climate. Due to human activity, greenhouse gas concentrations in the atmosphere are rising, which is causing significant changes in global temperatures and overall climate patterns (IPCC, 2019). Global temperatures are expected to rise by 3–5°C in the next 50–100 years, and experts expect to see an increased frequency of extreme weather events like drought and high temperatures (IPCC, 2014, 2019). Therefore, crops need to become more productive in increasingly challenging environments to keep up with global demand.

Environmental stress tolerance is a key factor for crop productivity, as abiotic stress is a major cause of reduced crop yields across the globe (Atkinson & Urwin, 2012). Abiotic stresses are estimated to reduce average yields by more than 50% for many major crops since they can have an adverse impact on nearly all stages of plant growth and development, causing leaf damage, accelerated leaf

senescence, reduced photosynthetic capacity, and greatly reducing plant biomass and grain production and therefore economic yield (Allakhverdiev et al., 2008; Atkinson & Urwin, 2012; Farooq et al., 2011). This means that there will be an ever-growing demand for stress-tolerant varieties as climate change brings with it more of these biomass- and yield-reducing stresses. To meet this demand, it is important to study plant responses to abiotic stresses.

Single abiotic stresses are more often studied than stresses in combination (Atkinson & Urwin, 2012; Rasmussen et al., 2013; Rizhsky et al., 2004). However, plant response to combinations of abiotic stress can result in transcriptional changes that differ from the simple summation of each individual stress (Rasmussen et al., 2013; Rizhsky et al., 2002, 2004). It is not surprising that plants have distinct responses to combined stress conditions in comparison to individual stresses, since many frequently co-occurring stresses can result in contradicting plant responses (Anderson et al., 2004; Asselbergh et al., 2008; Atkinson & Urwin, 2012; Balfagón et al., 2020; Choudhury et al., 2017; Mittler, 2006; Mittler & Blumwald, 2010; Suzuki et al., 2016). For example, a common response by plants under drought stress is closing stomata to preserve water, but in heat stress plants may open stomata to cool leaves and prevent tissue damage (Rizhsky et al., 2004). This means that in the combination of both drought and heat stresses, plant responses could look vastly different than when exposed to one of these stresses alone. Therefore, it is imperative to study not only plant responses to individual stresses but also responses to combinations of stresses to work towards developing new crop varieties. Since many major crops have been bred for high yield but not necessarily for abiotic stress tolerance, it is valuable to explore and exploit the natural diversity of stress tolerance in weedy relatives to current elite crops to understand plant abiotic stress responses (Mickelbart et al., 2015).

Brachypodium distachyon is a weedy Pooid C_3 grass that is closely related to important monocot food crop species including wheat, barley, and rice (International Brachypodium Initiative, 2010). *B. distachyon* also has a very similar cell-wall composition and overall architecture to major bioenergy grasses such as miscanthus and switchgrass (Coomey & Hazen, 2015; Gomez et al., 2008). In addition to these genetic or morphological similarities to major food and bioenergy crops, *B. distachyon* has a small stature, short generation time, is easy to cultivate and transform, and has extensive genomic resources available, which all combine to make it a very powerful and attractive model plant (Brutnell et al., 2015; Kellogg, 2015; Mur et al., 2011). *B. distachyon* accessions have been collected throughout its native growth range in the Mediterranean and the Middle East (Draper et al., 2001; Filiz et al., 2009; Garvin et al., 2008; Tyler et al., 2016). As is the case for many species, the reference accession of *B. distachyon* (Bd21-0), is not necessarily one with ideal responses to abiotic stress conditions, and relatively few studies have examined the phenotypic variation in other *B. distachyon* accessions under the same conditions (Benavente et al., 2013; Cao, Jiang, et al., 2016; Cao, Xu, et al., 2016; Chen & Li, 2016; Colton-Gagnon et al., 2014; Des Marais et al., 2017; Jiang et al., 2017; Liu & Chu, 2015; Luo et al., 2011; Rivera-Contreras et al., 2016; Shaar-Moshe et al., 2017, 2019; Shi et al., 2015; You et al., 2015). Even fewer studies have examined *B. distachyon* accessions under combinations of stresses, which, as mentioned earlier, is necessary to get a more representative picture of how *B. distachyon* would respond to stress in the field or in the wild (Chen et al., 2018; Cheng et al., 2018; Des Marais et al., 2017; Shaar-Moshe et al., 2017, 2019).

A brief review of *B. distachyon* literature demonstrates additional challenges in studying abiotic stress, and more specifically drought, as the same accessions are conflictingly described as drought tolerant or drought susceptible in different studies. In 2011, Luo et al. classified the *B. distachyon* reference accession, Bd21-0, as susceptible to drought stress compared to 56 others, and also described Bd1-1 as a drought-tolerant accession (Luo et al., 2011). Shi et al., on the other hand, identified Bd21-0 as being tolerant to drought (Shi et al., 2015), and Des Marais et al. examined both heat and drought stress and their combinations and identified Bd1-1 to be one of the lowest-yielding accessions under all combinations of drought and heat conditions tested (Des Marais et al., 2017). Less is known about the heat tolerance of these lines, but Des Marais et al. found that Bd21-0 had higher seed yield in hot but ample water conditions (Des Marais et al., 2017).

Conflicting results on the same accessions underline the difficulty in studying drought and could be partially due to the variety of ways in which drought can be applied and defined in experiments. Experimental application of water-limitation (drought) can differ greatly, which complicates the ability to directly compare results between studies. Acute drought stress can be applied by completely removing a plant from soil or growth media (Gagné-Bourque et al., 2015; Legnaioli et al., 2009). Progressive drought treatments can be applied by *maintaining* reduced watering levels compared to a control level over a longer period of time (Fahlgren et al., 2015; Granier et al., 2006; Skirycz et al., 2011). In a different kind of progressive drought treatment, water is withheld, allowing the soil to dry over time (Des Marais et al., 2017; Jiang et al., 2017; Luo et al., 2011; Shi et al., 2015). Progressive drought treatments are generally more representative of drought in the field than acute drought stress treatments are, but can often be more challenging to reproduce, since manually maintaining a specific reduced level of soil moisture is labor-intensive, and the severity of the drought stress depends on the consistency of soil drying between

replicates and experiments (Claeys & Inzé, 2013; Sun et al., 2014; Zhang et al., 2004).

Similarly, there are diverse ways to apply heat stress to plants, which again makes it difficult to compare results across different experiments. Acute heat stress is often applied by exposing plants to high temperatures for a relatively short period of time (generally a few hours) and then taking measurements for traits of interest directly after the heat treatment (Sun et al., 2017). Progressive heat treatments are often done by maintaining high ambient temperatures for the entire course of the experiment at some point after germination (Des Marais et al., 2017; Fahlgren et al., 2015; Hedhly et al., 2020). Alternatively, exposing plants to high heat every day for a certain length of time can be used to simulate a common form of progressive heat stress in the field (Samakovli et al., 2020).

To address issues of inconsistency, reproducibility, and high labor input requirements in implementing abiotic stress treatments, automated watering and growth systems have been developed. Within the last decade, these automated systems in greenhouses, growth chambers, and experimental fields have advanced considerably, making it possible to apply abiotic stress treatments reproducibly at the population scale (Chen et al., 2014; Fahlgren et al., 2015; Granier et al., 2006; Skirycz et al., 2011). This study uses an automated watering and image-capture system to apply combinations of drought and heat stress to a diverse population of *B. distachyon* accessions in two experiments. Since imaging is a non-destructive measurement, assessing stress through image data allows the progression of stress to be tracked over time.

To analyze image data from these two experiments under combinations of drought and heat stress, this project utilizes high-throughput image analysis tools. The field of image-based high-throughput phenomics develops methods to capture, extract, and utilize plant trait information over time from image data. PlantCV is an open-source, open-development image analysis package written in Python that enables users to develop image processing workflows, then parallelize those workflows over large sets of image data (Fahlgren et al., 2015; Gehan et al., 2017). This software has been used to extract numerical data from images to estimate various traits, including biomass (Fahlgren et al., 2015) and plant health (Enders et al., 2019; Zheng et al., 2019) for various plant species (Gehan et al., 2017).

In this study, numerical trait information extracted from image data, along with new low-coverage sequencing data for *B. distachyon*, is used to carry out a genome-wide association study (GWAS). A GWAS allows the identification of genetic polymorphisms that are found more frequently in organisms with the trait being assessed (Ingvarsson & Street, 2011; Wilson et al., 2015). GWAS can be used to explore the genetic architecture of complex traits in plants, identifying the number of alleles, genetic loci, and effect sizes associated with a certain phenotype (Ingvarsson & Street, 2011; Wilson et al., 2015). Complex traits would normally be difficult to examine without GWAS, since many adaptive traits are influenced by many genes that each individually have a small to moderate effect on the phenotype (Ingvarsson & Street, 2011). This is true for plant responses to drought and heat stresses, which are polygenic and not as easily isolated and identified as discrete traits like flowering time (Tyler et al., 2016). Thousands of GWAS have been conducted in major crops such as rice, wheat, maize, and sorghum, which have included a variety of traits examining everything from yield to plant development to characteristics associated with biotic and abiotic stresses (Gupta et al., 2014, 2019). Genetic loci of interest identified in a GWAS can be used to develop improved cultivars through traditional breeding methods or through genetic engineering (Gupta et al., 2019). One important documented example of the use of GWAS results to improve a major crop was the development of a line of maize with increased pro-vitamin A content (Xiao et al., 2017).

There have been a few GWAS done in *B. distachyon*, but compared to major crop species and other important model plants, the genetic architecture of *B. distachyon* remains relatively unexplored (Dell'Acqua et al., 2014; Lee, 2016; Tyler et al., 2016; Wilson et al., 2015, 2019). Multiple studies have identified genetic loci associated with flowering time in. *B. distachyon* (Tyler et al., 2016; Wilson et al., 2019), others have explored genetic loci associated with environmental adaptation or fitness in their different climates of origin (Dell'Acqua et al., 2014; Wilson et al., 2015), and genetic loci associated with biofuel-related traits such as biomass accumulation have also been identified (Lee, 2016; Wilson et al., 2019), but not under abiotic stress.

In this study, the diversity and natural variation of a diploid *B. distachyon* population of 149 accessions under combinations of progressive heat and drought stresses are examined. These accessions were originally collected throughout the native growth range of *B. distachyon*, and come from diverse climates of origin with a wide range of elevations, temperatures, and precipitation patterns (Figure 1; Data S1) (Mur et al., 2011; Vogel et al., 2009). At this time, this is the largest temporal phenotypic assessment of this crucial model plant to date and also provides the community with additional low-coverage sequencing information because 132 of the accessions used in this study do not overlap with the accessions genotyped in Tyler et al. (Tyler et al., 2016). A GWAS was performed to investigate the underlying genetic architecture in *B. distachyon* that is associated with changes in plant phenotype in each of the drought and heat stress conditions, which will also provide new information about the *B. distachyon* genome and its involvement in abiotic stress responses. This study

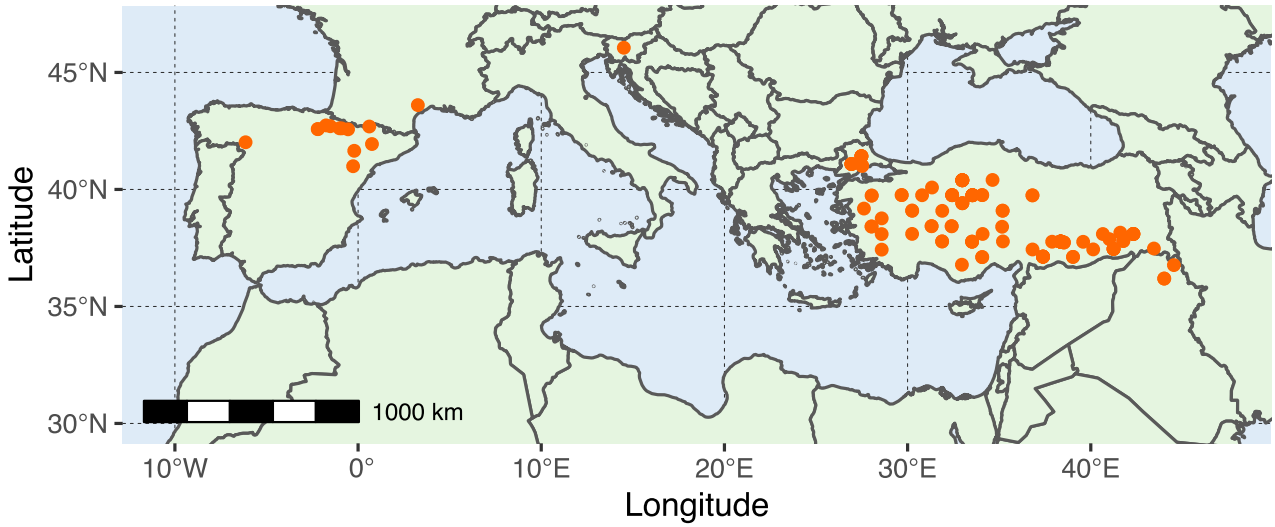

Figure 1. Map of *B. distachyon* collection locations for accessions used in this studyMap of Southern Europe, Northern Africa, and the Western Middle East showing the distribution of collection locations of 147 of the *B. distachyon* accessions included in this study (specific collection location is unavailable for two of the 149 accessions) (Draper et al., 2001; Filiz et al., 2009; Garvin et al., 2008; Tyler et al., 2016). The x- and y-axes represent longitude and latitude on the Earth's surface, respectively. The scale bar in the bottom left represents 1000 km.

examines *B. distachyon* as a model for bioenergy grasses, so the focus traits are biomass accumulation, plant height, and percent of 'healthy' tissue under stress conditions.

RESULTS

Experimental overview

To examine the natural variation of *B. distachyon* under drought, heat, and combined drought and heat, low-coverage sequencing data (genotyping-by-sequencing; GBS) and two high-throughput phenotyping experiments using the Bellwether Phenotyping Platform at the Donald Danforth Plant Science Center (Fahlgren et al., 2015) were done (Figure 2). In the first phenotyping experiment (Figure 2a), 137 *B. distachyon* accessions were grown under control or water-limited conditions (20% of control watering, starting on day 5 on the phenotyping platform). In the second experiment (Figure 2b), a mostly overlapping population of 144 *B. distachyon* accessions were treated with heat or both heat and water-limited conditions (20% of control watering, starting on day 5 on the phenotyping platform). Because the Bellwether Platform growth chamber is not subdivided to accommodate two different temperature conditions, the two temperature treatments could not be done simultaneously. Plant growth conditions were kept as similar as possible between the two experiments, with the only major difference being the temperature (Figure S1). Plants were imaged every other day throughout both experiments, which totaled 148 491 side-view RGB images. To account for any differences between the images from the two experiments, the images from each experiment were processed independently and the normalized outputs were compared. This project utilizes the high-throughput plant phenomics software PlantCV (Fahlgren et al., 2015; Gehan et al., 2017). The Experimental

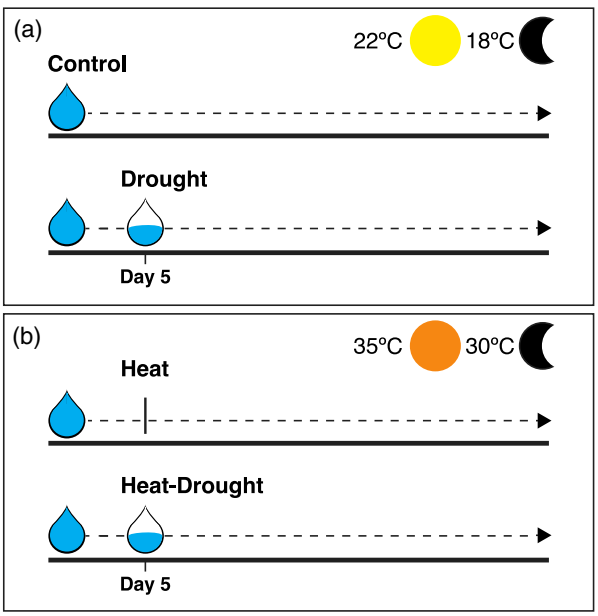

Figure 2. Experimental conditions for phenotyping experimentsExperimental conditions for both experiments were conducted. A) Experiment with control and drought treatments. Both were grown at 22°C during the days and 18°C during the nights, with the drought-treated plants receiving 20% of control watering starting on day 5 on the phenotyping platform. B) Experiment with heat and a combination of heat and drought treatments. Both were grown at 35°C during the day and 30°C during the night, with heat and drought combination treated plants receiving 20% of control watering starting on day 5 on the phenotyping platform (heat treatment began on the same day). All plants were grown under a 14 h photoperiod.

Procedures section provides a more detailed description of the analysis methods and links to data.

Individual and combined abiotic stress treatments can be differentiated by PCA over time

A principal component analysis (PCA) was used on data for 13 traits extracted from images with PlantCV (percent_damage, area, height_above_reference, hue_circular_mean, width, height, convex_hull_area, solidity, perimeter, longest_path, ellipse_major_axis, ellipse_minor_axis, ellipse_angle, ellipse_eccentricity) to assess the effects of the different treatment conditions in this study (Figure 3). The PCA analysis shows the overlap of all experimental conditions at 16 days after planting (DAP), which is prior to the application of different treatments, indicating that despite the separate experiments, no substantial phenotypic differences between plants were discernible before stress treatments began. Over the subsequent days of the experiment, the different treatment groups begin to separate based on their phenotypic differences, and by 44/45 DAP (the final days of the experiments with complete data), the PCA results show strong separation between most treatments (Figure 3). It is noteworthy that there is a strong separation between the drought (yellow) and heat (blue) treatments as well as drought (yellow) and heat-drought (green) treatments, but there is still substantial overlap between the heat (blue) and heat-drought (green) treatment groups (Figure 3).

Heat stress alone resulted in the most tissue damage in comparison to drought and the combined stress

The naïve Bayes classifier from PlantCV calculates the statistical likelihood that a pixel belongs to user-defined classes (Abbasi & Fahlgren, 2016; Gehan et al., 2017). To estimate the effects of individual and combined drought and heat stresses on tissue damage in *B. distachyon*, two classes of healthy and unhealthy tissue were defined based on color. The amount of unhealthy tissue was then calculated as a percentage of the total plant shoot area identified, and categorized as 'percent damage'. When examining these data across the *B. distachyon* population, there is considerable variation in response to the different stress treatments (Figure 4). When compared to the control, some accessions, such as BdTR10E and BdTR9K, can maintain relatively low percentages of damage across all three stress treatments, while others, such as BdTR2G, have relatively high percentages of damage across the stress treatments compared to control (Data S2). On the other hand, certain accessions have high percentages of damaged tissue in some stresses but not in others. For example, Adi-4 has among the highest increase in percent damage in heat and heat-drought, but among the lowest in the drought treatment, whereas ABR6 and BdTR9I have among the highest increase in percent damage in the drought and heat-drought treatments, but among the lowest in the heat treatment (Data S2). An unexpected result when looking at the percent damage on these plants was that heat stress alone seems to have caused the most estimated tissue damage in comparison to drought or the combined stress (Figure 4). The mean percent damage in heat, 33.7%, is about double the mean percent damage in drought, 17.0%, and the heat-drought combination, 14.2%, and many accessions have far more estimated tissue damage under heat than under drought or heat-drought. The mean increase in percent damage between control and heat is 23.2%, while it is only 6.3% in drought and 3.4% in heat drought. BdTR5J is an example of an accession that follows this trend, having nearly 100% damaged tissue under heat stress, but remaining relatively healthy under drought and heat-drought conditions (Figure 5). Bd21-0, which is often used as a reference line for *B. distachyon*, also follows this trend and has almost double the percent damage in heat compared to both drought and the heat-drought combination (Data S2). BdTR10E is an example of one of the few accessions not following this trend and maintains healthy, green tissue under all three stress treatments (Figure 5).

The combination of heat and drought stresses resulted in the greatest decrease in biomass compared to heat or drought alone

PlantCV outputs were also used to examine biomass accumulation of *B. distachyon* in these abiotic stress treatments by assessing both image-estimated plant height and plant shoot area. Heatmaps of plant height show that while there is variation across the accessions, the majority are still able to grow relatively tall in the drought treatment compared to the other stresses, especially in comparison to the combination of heat and drought (Figure 6). A similar pattern is seen for the plant shoot area (above-ground area) across treatments and accessions (Figure S2). Two accessions, Adi-8, and BdTR2B, show robust growth under these stress conditions, as they have among the smallest decrease in area and height compared to the control (Data S2). Conversely, accessions such as BdTR11A and ABR5 were among the worst of all accessions across stress treatments for biomass robustness, with large decreases in area and height under all stresses assessed (Data S2). The commonly used reference accession, Bd21-0, was also much smaller in size under all stress treatments compared to the control (Data S2). Overall, the combination of drought and heat stresses seems to have a more detrimental impact on biomass accumulation than heat or drought stress individually, though heat alone is a close second (Figure 6; Figure S2). This suggests that *B. distachyon* has non-overlapping responses that decrease biomass accumulation when exposed to the combination of drought and heat stress in comparison to individual stresses. Additionally, these data seem to indicate that heat caused a more

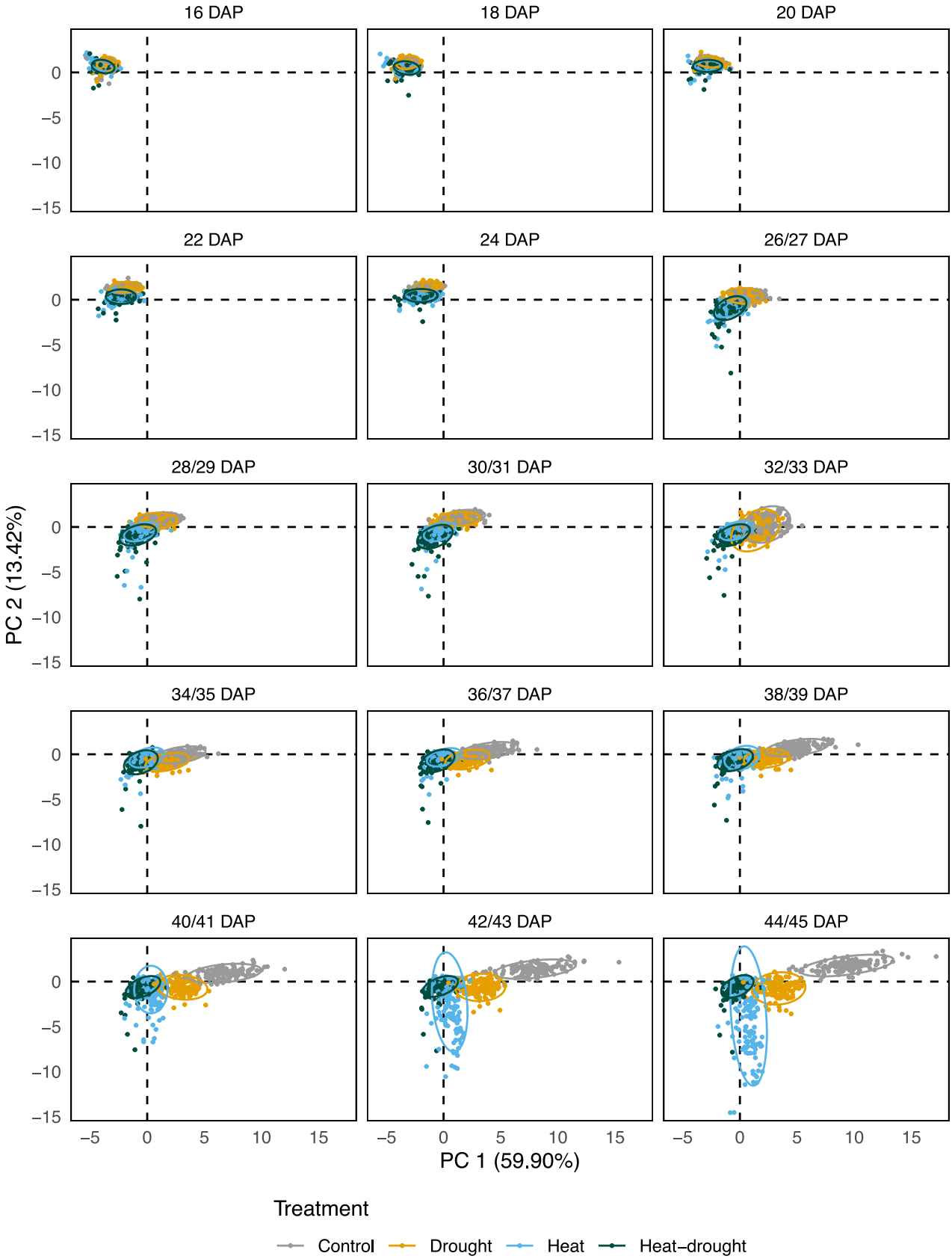

Figure 3. PCA of phenotypes measured with PlantCV Principal component analysis of *B. distachyon* responses to different experimental conditions over time using trait data extracted from images with PlantCV. Data are organized by days after planting (DAP). Traits included are: percent_damage, area, height_above_reference, hue_circular_mean, width, height, convex_hull_area, solidity, perimeter, longest_path, ellipse_major_axis, ellipse_minor_axis, ellipse_angle, ellipse_eccentricity. The graph shows principal component 1 (PC 1) on the *x*-axis, which explains 59.90% of the variance, and principal component 2 (PC 2) on the *y*-axis, which explains 13.41% of the variance, with 95% confidence ellipses included. Points are colored by treatment.

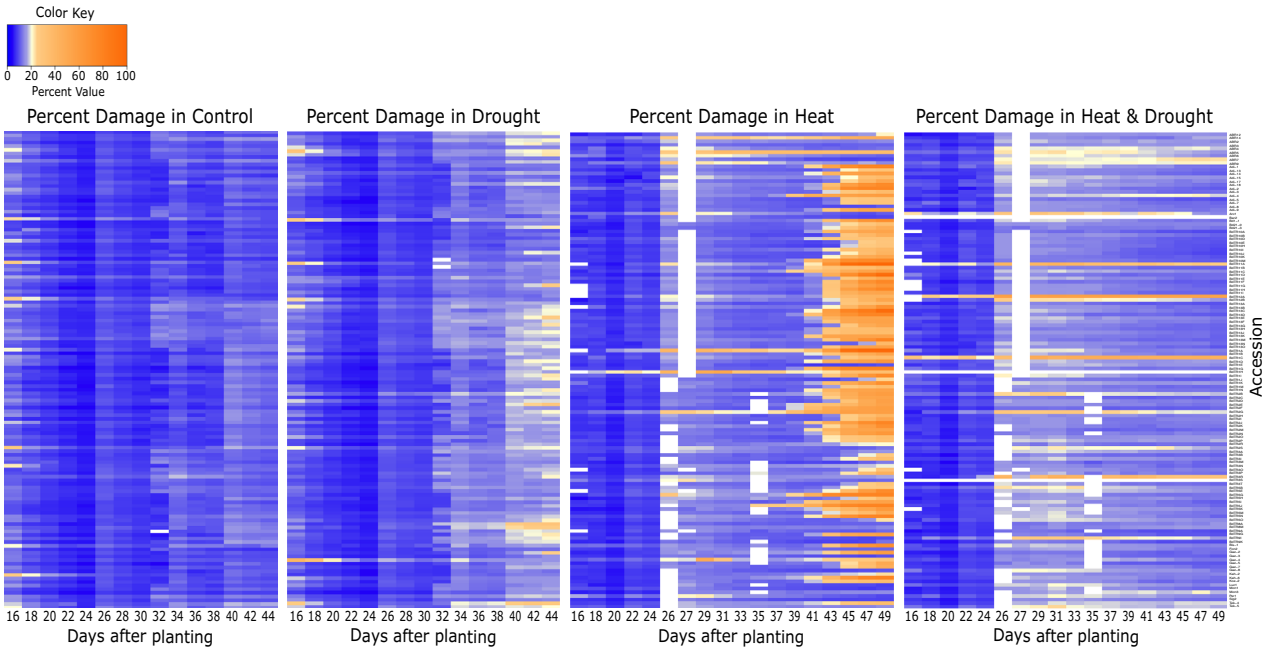

Figure 4. Heatmaps of percent damage of plant tissue throughout the experimentsHeatmaps of the average percentage of damaged tissue in plants from the naïve Bayes classifier, in the four experimental conditions (from left to right: control, drought, heat, heat & drought combined). This was calculated by taking the mean of the percent damage of all plants of the same accession in the same treatment on each day they were imaged. The *x*-axis of each heatmap shows days after planting (DAP). On the *y*-axis are the accessions, sorted alphabetically in descending order. White boxes indicate missing data. Common color key for all treatments in the top left; blue indicates plants with lower estimated percentage of damaged tissue, and orange indicates plants with higher estimated percentage of damaged tissue.

extreme biomass reduction compared to drought, since the plants were generally able to maintain biomass in the drought treatment but were considerably smaller in both the heat and heat-drought treatments. However, although plants are smaller under the combined stress conditions, the results from the naïve Bayes classification would suggest that they have a lower percentage of damaged tissue. Therefore, *B. distachyon* maintains a higher amount of healthy, undamaged tissue under the combined stress in comparison to heat stress alone, which would suggest that *B. distachyon* is better able to respond to the combination of heat and drought stresses.

Identification of stress-tolerant and stress-susceptible accessions

The focus of this study was to assess the natural diversity in *B. distachyon* resilience to drought and heat stresses. The aim was to identify accessions with resilient growth across multiple stresses – not only in one stress – so here accessions are identified as stress-tolerant only if they perform well in all three stress conditions, and susceptible if they perform poorly in all stresses.

There are a variety of ways to assess resilience under stress conditions. Taking the difference between an accession's performance under stress and in control can show how its size or health changes in a stress condition compared to control. However, this measurement does not take into account the size of the plant in control conditions. An accession may have a very small reduction in size between control and the stress treatments, but this plant could also be one of the smallest accessions in control, to begin with. Therefore, just looking at the difference between stress and control can be misleading, because small changes in size in a large plant would be a much smaller percent change than the same numerical difference in a smaller plant. Accordingly, assessing the difference in height and area between plants grown under stress conditions and control conditions relative to the size in control makes it possible to accurately compare accessions. This is not necessary for the percent damage phenotype, as this is

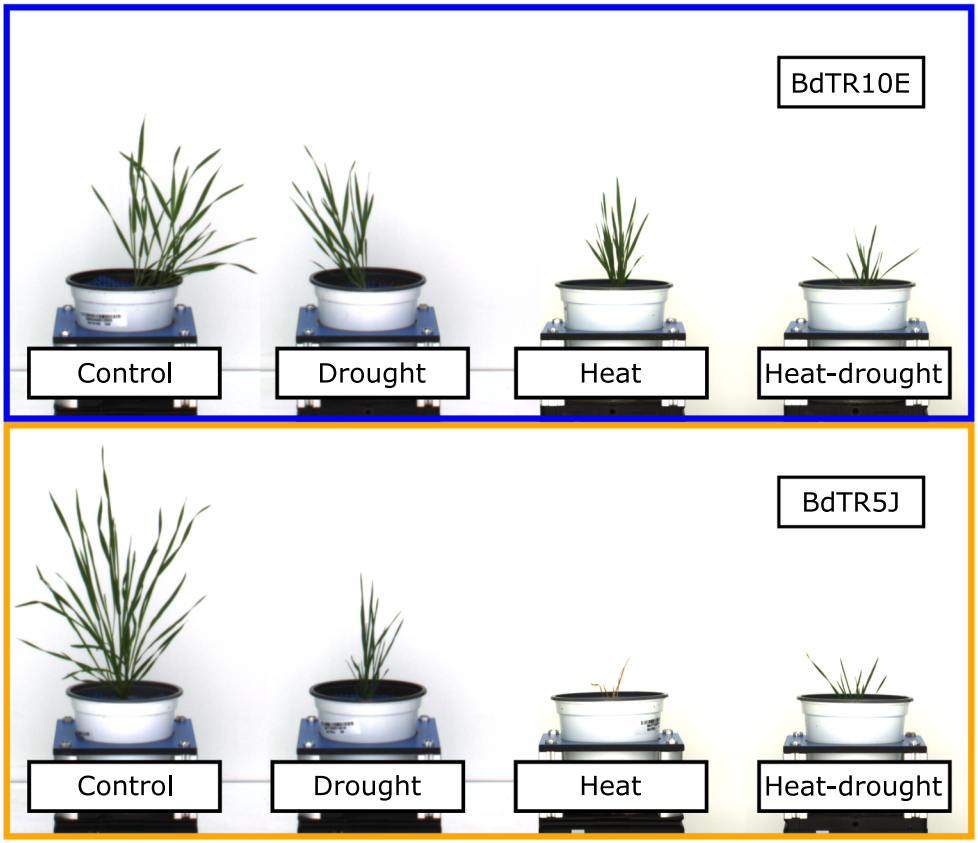

Figure 5. Images of stress-tolerant and susceptible accessionsPanels showing images of plants from two *B. distachyon* accessions in all four treatments. The top, outlined in blue, shows accession BdTR10E, which has been classified as a stress-tolerant accession, and the bottom, outlined in orange, shows accession BdTR5J, which has been classified as a stress susceptible accession.

already a percent. The area, height, and percent damage of the accessions in all four growth conditions of this study were used to assess overall accession performance across the treatments. Since the goal of this study is to identify accessions that display resilient or robust growth across the stresses assessed, the growth under stress conditions is always evaluated relative to the growth under control conditions by using the percent change between the trait in control and the stress treatments. Since these three traits (area, height, percent damage) are all on different scales, these values needed to be normalized to be able to compare across traits and treatments. A z-score, also known as a standard score, is a method of describing a value's distance from the mean of a group of values (how many standard deviations from the mean the value is) and can be used to compare values across datasets with different scales. Z-scores were calculated for the measurements in control, as well as the percent change between the stresses and control for these traits. These z-scores were included in heatmaps examining resilience in accession area, height, and percent damage on the final day of the experiments across all four experimental conditions. The accessions were ordered using the mean of the z-scores for all three traits (area, height, percent damage) in the four experimental conditions to rank them by performance across stresses and traits (Figure 7). Accessions with the smallest deficits in plant size and health compared to control conditions were identified as having resilient growth under stress, while accessions with the biggest decreases in size and healthy tissue under stress conditions compared to control were identified as not having resilient growth under these stresses. An ideal, stress-tolerant plant, would grow large and healthy in control conditions, and experience very limited reduction in size and health under stress. In the context of biofuel production, larger, healthier plants are most desirable as they will result in the greatest biomass yield per plant. So, even if an accession has similar growth to control under stress conditions, if the accession grows relatively poorly under control conditions to other accessions, it would not be considered ideal. Under these tested environments, it seems that the accessions that are the largest and healthiest in control are not very resilient to the heat and drought stresses assessed (Figure 7). The accessions that are biggest in the control

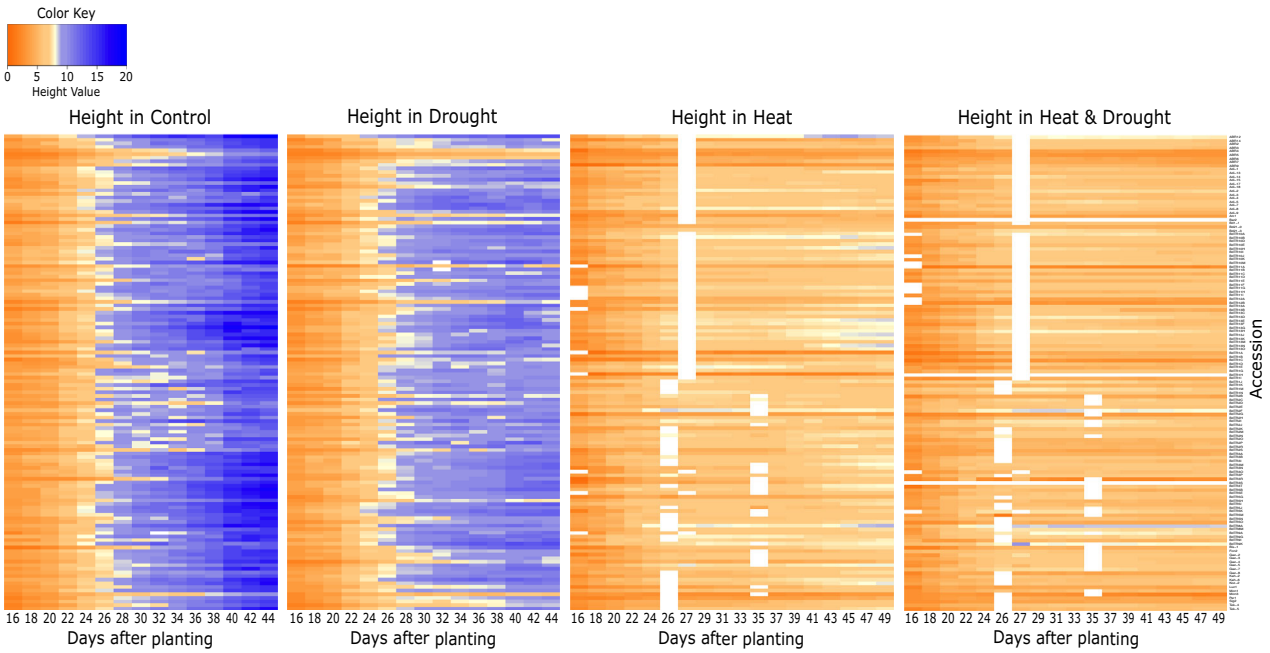

Figure 6. Heatmaps of plant height throughout the experimentsHeatmaps of average plant height in the four experimental conditions (from left to right: control, drought, heat, heat & drought combined). This was calculated by taking the mean height (height_above_reference from PlantCV) of all plants of the same accession in the same treatment on each day they were imaged. The *x*-axis of each heatmap shows days after planting (DAP). On the *y*-axis are the accessions, sorted alphabetically in descending order. White boxes indicate missing data. Common color key for all treatments in top left; orange indicates shorter plants, and blue indicates taller plants.

treatment in these heatmaps generally have a much higher relative decrease in size and health across the stress conditions. Whereas, the more average-sized accessions in control seem to have more resilient growth under these stresses (Figure 7). Many accessions had resilient growth in specific stresses but not in others, but there were a few accessions that consistently performed well or poorly. BdTR10E and BdTR9K were the two accessions identified as being most resilient, and therefore tolerant, to the assessed stress conditions. Both accessions had about the average area, height, and percent damage in control, but then among the lowest decreases in size and increases in percent damage across the stress conditions, indicating resilient growth to these stresses relative to the other accessions in this study (Figure 7). On the other hand, BdTR2G and BdTR5J, are among the least resilient accessions, and therefore most stress susceptible, with some of the largest relative decreases in size and increases in percent damage in the stresses compared to control (Figure 7). Images of BdTR10E, a tolerant accession, and BdTR5J, a susceptible accession, show how these differences in stress tolerance are reflected in *B. distachyon* appearance under these stress treatments compared to the control (Figure 5).

While the goal was to identify accessions with resilient growth across all stress conditions, in particular, it is still useful to identify accessions that are especially tolerant or susceptible to single stress treatment. The normalized values (z-score) for the trait measurements in control and the difference between the stresses and control were used here as well. Accessions were ranked by mean values of z-scores for all three traits (area, height, percent damage) in each treatment to find accessions that have resilient or poor growth across the three traits within each stress. Complete lists of the accessions ranked by performance in each of the stresses can be found in the Supporting Information (Data S2). A notable result is that Bd21-0, a commonly used reference line for *B. distachyon*, performed very poorly in the heat and heat-drought combination stress treatments (Data S2). Bd21-0 is just above average in the drought stress but is in the bottom 25% of accessions in the heat and heat-drought treatments (Data S2).

Variance explained by treatment is larger and appears earlier in heat and heat-drought treatments than in drought

For each stress treatment compared to control, the partial correlations, or percent variance explained, of genotype, treatment, and the genotype-treatment interaction (GxE) were calculated using a variance components model. The analyses were done using data from four time points throughout the experiments, corresponding to 22, 28/29, 36/37, and 44/45 DAP, to assess the variance explained over time. The variance explained was plotted in stacked bar graphs to show both the total variance explained for

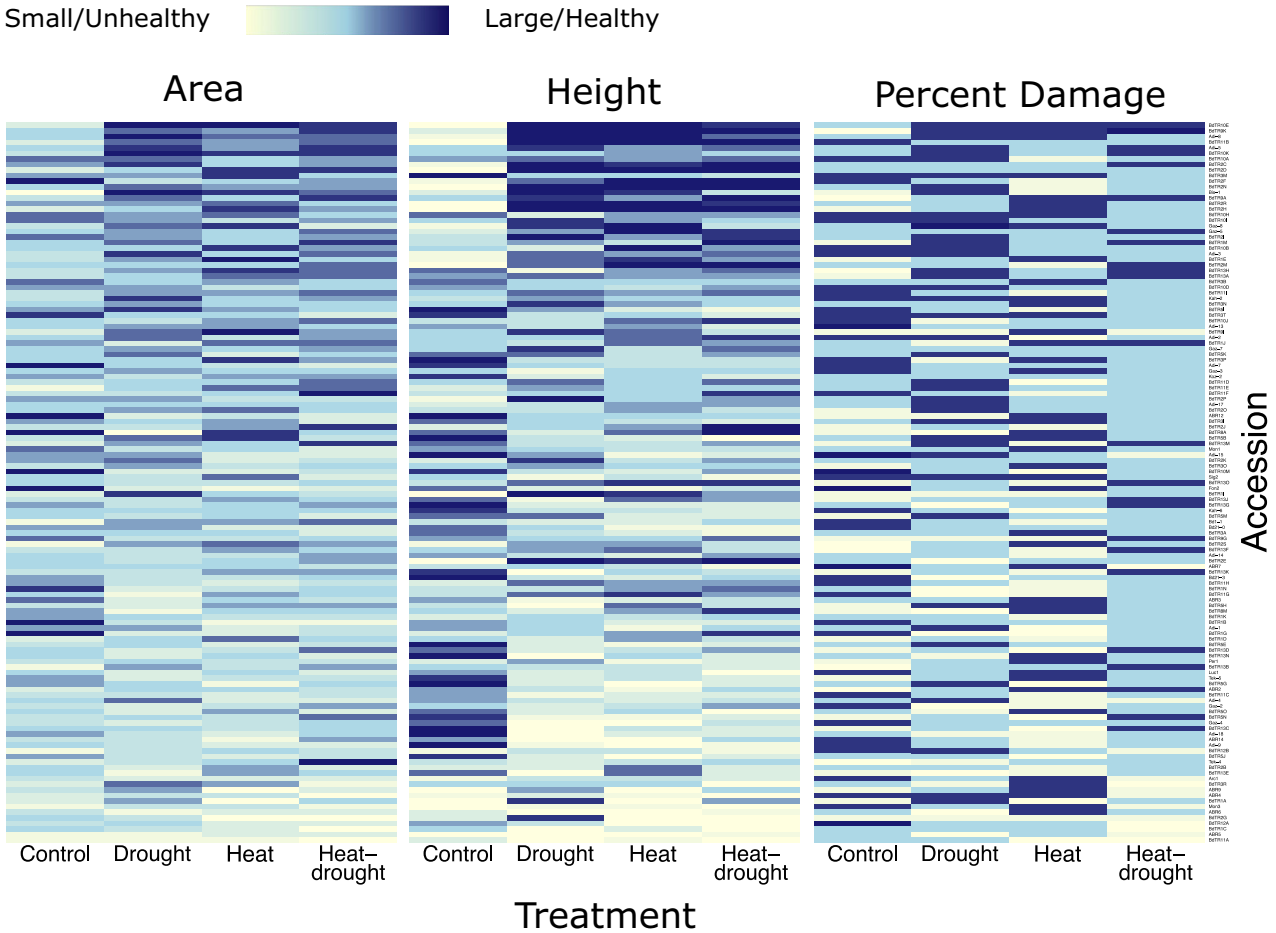

Figure 7. Heatmaps of accession performance in stress treatmentsHeatmaps of z-score values for plant area, height, and percent damage in control and the percent change between control and the three stress treatments at 44/45 DAP. The *y*-axis shows the accessions, ranked in descending order by the mean of the z-scores across all four treatments for all three traits. The *x*-axis shows the treatments, and the color indicates 'performance' in the treatment, with lighter colors indicating 'poor' performance (small area or height, or large percent damage), and darker colors indicating 'good' performance (large area or height, small percent damage).

each phenotype measured as well as the amount explained by genotype, treatment, and the genotype-treatment interaction, in addition to the amount unexplained (Figure 8). These values are also available in the Supporting Information (Data S3). The variance explained by the genotype represents the broad sense of heritability of the traits among these *B. distachyon* accessions. For most traits, the genotype components were largest at Time Point 1 and decreased over time as the treatment effect increased (Figure 8). This is especially true for the drought treatment, where the treatment component only begins to account for any meaningful portion of the variance explained in Time Point 2. In the heat and heat-drought treatments, however, the treatment component accounts for a much larger portion of the variance explained earlier, with this component making up over 70% of the variance explained for some variables already at Time Point 1 in both the heat and heat-drought treatments, compared to less than 1% in the drought treatment. Additionally, the variance explained by the treatment is larger overall in the heat and heat-drought treatments compared to the drought treatment. The largest is 89.37% and 89.96% for any variable in the heat and heat-drought treatments, respectively, at Time Point 4, compared to 79.26% in the drought treatment (Figure 8). This suggests that the heat treatment impacted plants earlier than the drought treatment, which is likely because the water-limitation treatment started with soil at well-watered levels, and therefore would take time to dry down to target levels, while the increase in temperature was immediate. Also, since the traits in both treatments that involve heat (heat and heat-drought) have higher percentages of their variance explained by the treatment, in contrast to the drought treatment, this demonstrates that the responses to the heat treatments are more severe compared to the responses to drought for the *B. distachyon* accessions in this study.

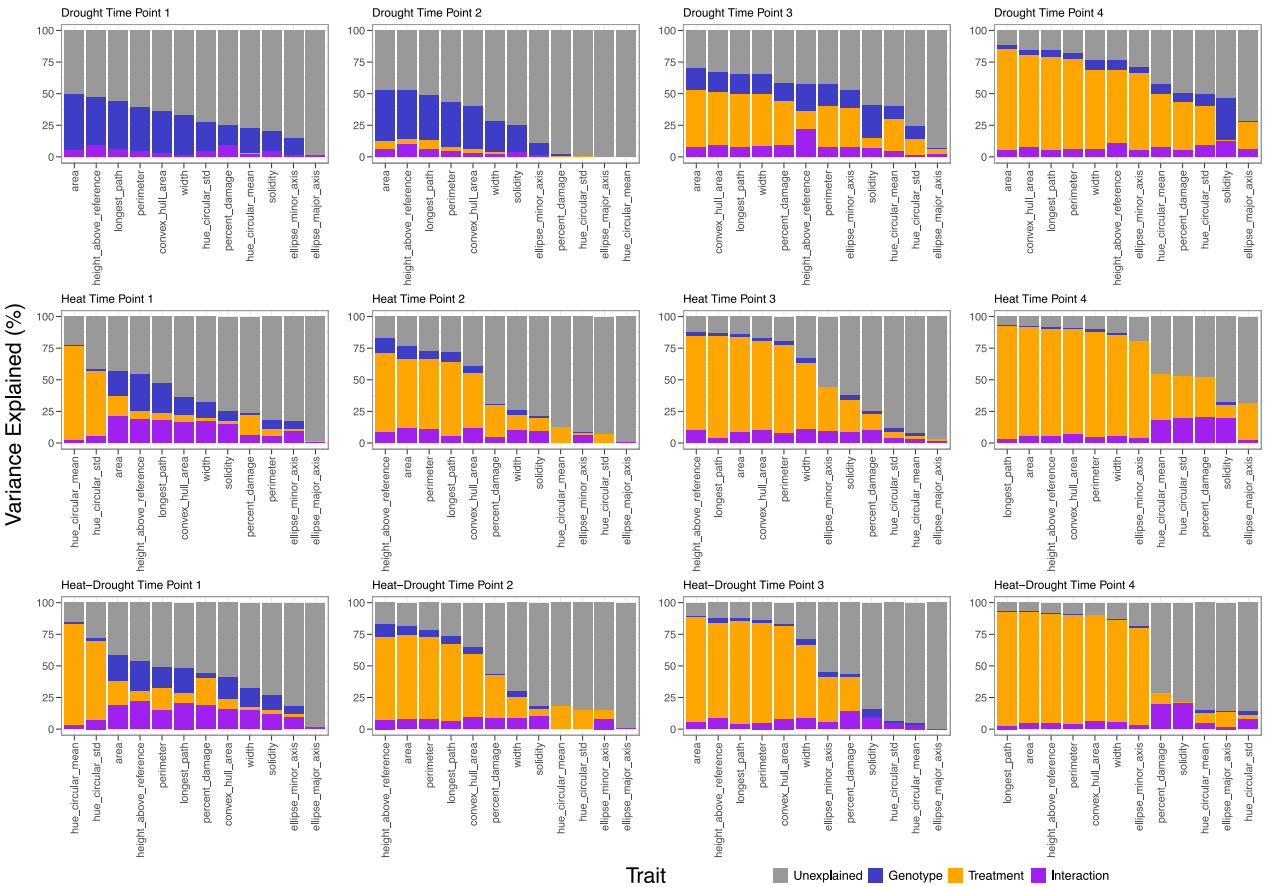

Figure 8. Percent variance explained by genotype, treatment, and genotype-treatment interactionStacked bar graphs of the variance explained between all stress treatments compared to control conditions. The x-axes show different phenotypic measurements output from PlantCV, and the y-axes show the percent variance explained. Gray bars represent unexplained variance, blue bars represent variance explained by genotype, orange bars represent variance explained by treatment, and purple bars represent variance explained by genotype-treatment interaction. The top row shows the variance explained between control conditions and the drought treatment. The middle row shows the variance explained between control conditions and the heat treatment. The bottom row shows the variance explained between control conditions and the combined heat and drought treatment. Plots are organized by time point in columns, Time Point 1 is 22 days after planting (DAP), Time Point 2 is 28/29 DAP, Time Point 3 is 36/37 DAP, and Time Point 4 is 44/45 DAP.

B. distachyon has strong population structure with two main subpopulations separated based on country of origin

The data presented so far demonstrate that there are differences in phenotype between the *B. distachyon* accessions included in this study under the environmental conditions assessed. Investigating the underlying genetics could help elucidate what might be driving these phenotypic differences.

Population structure is the presence of a difference in allele frequencies between different groups in the population and it often arises from physical separation between members of a species either because of distance or barriers (Corander et al., 2008). Population structure is important to identify because it could lead to errors in genetic analyses like GWAS if a homogenous distribution of alleles throughout the population is incorrectly assumed (Corander et al., 2008). Using single nucleotide polymorphisms (SNPs) identified from the GBS data, a PCA was done to examine the population structure of the *B. distachyon* accessions in this study (Figure 9). PCA shows two main clusters (with a few accessions not in either cluster), which indicates that there is a strong population structure present in this population of *B. distachyon* accessions (Figure 9). These results support previous conclusions that found a strong population structure in *B. distachyon* populations (Draper et al., 2001; Filiz et al., 2009; Garvin et al., 2008; Tyler et al., 2016). Clustering is almost exclusively by country of origin, with accessions from Spain and Turkey making up the two main subpopulations (Figure 9). Fixation index (Fst) calculations between these two main subpopulations also confirmed the genetic separation between them (Weir and Cockerham mean Fst estimate = 0.4014). A kinship matrix visualizes how these subpopulations cluster by genotype (Figure S3).

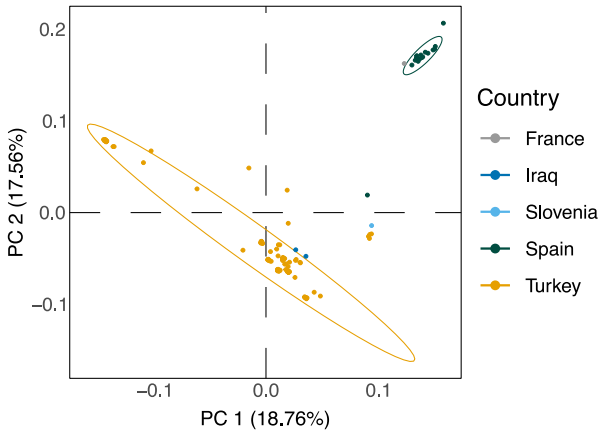

Figure 9. PCA of population structure for the *B. distachyon* accessions used in this studyPrincipal component analysis (PCA) of *B. distachyon* population structure. This PCA incorporates SNP information, called using Stacks, for 147 *B. distachyon* accessions. The graph shows principal component 1 (PC 1), which explains 18.76% of the variance, on the *x*-axis, and principal component 2 (PC 2), which explains 17.56% of the variance, on the *y*-axis, with 95% confidence ellipses included. Points are colored by the country of origin for each accession.

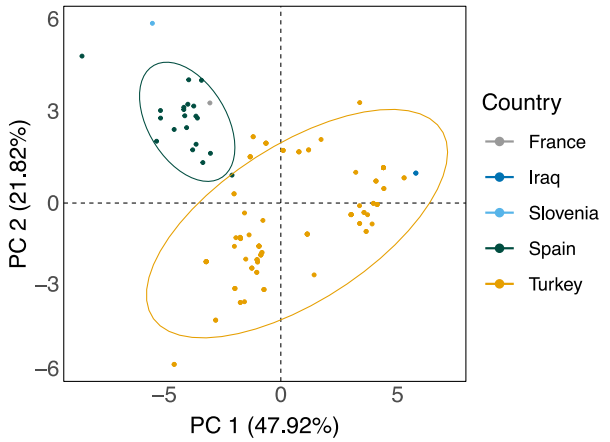

Figure 10. PCA of bioclimatic variables describing *B. distachyon* climate of originPrincipal component analysis (PCA) of *B. distachyon* collection location climates, using data downloaded from WorldClim. This PCA incorporates 19 bioclimatic variables describing in detail the climate in the location where 147 of the 149 *B. distachyon* accessions were collected, which we define as 'climate of origin' (specific collection location is unavailable for two accessions). The graph shows principal component 1 (PC 1), representing 47.92% of the variation explained, on the *x*-axis and principal component 2 (PC 2), representing 21.82% of the variance explained, on the *y*-axis, with 95% confidence ellipses included.

B. distachyon climate of origin is correlated with responses to heat and drought stresses

To see if there was a correlation between more 'stress tolerant' accessions and the climates that they were collected in, the correlation between the climate of each *B. distachyon* accession collection location (climate of origin) and its phenotypic response under stress was examined. Although the *B. distachyon* accessions assessed in this study are native to hot, arid regions of the world, there is still considerable variation between the climates of origin. Given the hypothesis that plants have adapted to the environment in which they have evolved (Anderson et al., 2011; Mitchell-Olds et al., 2007), the goal of this research was to determine if there were correlations between phenotype and climate of origin. Although we would need to explore these further, these correlations might suggest that local adaptations to different climates could be driving genetic and phenotypic differences in *B. distachyon*. Using data from WorldClim (Fick & Hijmans, 2017), 19 bioclimatic variables plus elevation data were included in this analysis. The data point from WorldClim that was closest to each accession's collection location was designated as that accession's 'climate of origin'. More detail about this process can be found in the Experimental Procedures section. A correlation plot of the bioclimatic variables shows strong correlations between different groups of variables, which help to describe general patterns in the climates of origin for the *B. distachyon* accessions (Figure S4). The correlations between the bioclimatic variables indicate that the accessions come from climates that are generally hot and dry, or cooler and wet at different times of the year. The strong positive relationships between Precipitation of Driest Month (bio14), Precipitation of Driest Quarter (bio17), and Precipitation of Warmest Quarter (bio18), as well as the strong negative relationship between Mean Temperature of Warmest Quarter (bio10) with the three previously mentioned precipitation-related variables (bio14, bio17, bio18), indicate that the warmest time of year in the climates of origin of this *B. distachyon* population coincides with the driest time of year (Figure S4). The strong positive correlation between Precipitation of Wettest Quarter (bio16) and Precipitation of Coldest Quarter (bio19) demonstrates that the wettest time of the year is also the coolest time of the year (Figure S4). As expected, higher elevations are associated with cooler temperatures in the *B. distachyon* climates of origin, as indicated by the negative relationship between Elevation and Annual Mean Temperature (bio1), Max Temperature of Warmest Month (bio5), Min Temperature of Coldest Month (bio6), Mean Temperature of Warmest Quarter (bio10), and Mean Temperature of Coldest Quarter (bio11) (Figure S4).

A principal component analysis (PCA) of climate data (19 bioclimatic variables from WorldClim) showed that climatic differences grouped by collection country of origin, are similar to the population structure clusters (Figures 8 and 10). Clear differences in climate of origin across the *B. distachyon* population explain a large portion of the variation across the climate variables (~ 70%; Figure 10). There were two main climate clusters, one mostly representing the *B. distachyon* accessions collected in Turkey (yellow

points; Figure 10) and the second clustering of the data points predominantly representing the accessions collected in Spain (green points; Figure 10). This separation suggests meaningful differences in the climates of these two native growth regions for *B. distachyon*. Over time, these climatic differences could contribute to selective pressures that drive differences in abiotic stress tolerance between *B. distachyon* accessions. Since only one accession from France and Slovenia, and two from Iraq have climate data available, there are not enough data to make conclusions about the climate of these regions compared to the others (Figure 10).

Further evaluation of the WorldClim data revealed significant correlations between climate of origin and *B. distachyon* responses to the abiotic stress conditions assessed (*P*-values <0.05, Spearman correlation test). A total of 14 bioclimatic variables from WorldClim and elevation, out of the 20 climatic variables assessed, are significantly correlated with *B. distachyon* responses to these stresses. The climatic variables are correlated with either height or percent damage in each of the three stress conditions, but no climate variables were significantly correlated with plant area (Figure 11). The relationships between the climate variables and plant traits are colored based on the correlation coefficient, and significant correlations are denoted with asterisks based on *P*-value (* $P < 0.05$, ** $P < 0.01$). Of the variables that are correlated with the *B. distachyon* response to the stresses assessed, seven are associated with only one stress condition. There is just one variable – bio5, the max temperature of the warmest month – that is correlated with only drought, and also just one – bio16, precipitation of wettest quarter – that is only correlated with heat, while there are five variables that are only correlated with the heat-drought combination (Figure 11). On the other hand, eight variables are associated with more than one stress. Two of these – bio3, isothermality (mean of monthly temperature range/temperature annual range), and bio12, annual precipitation – are significantly correlated with *B. distachyon* response to all three stress conditions: drought, heat, and the combination of drought and heat (Figure 11). These correlations suggest that there are significant relationships between the climate of origin and *B. distachyon* phenotype in abiotic stress conditions, which could indicate local adaptation that is driving the diverse stress responses of these accessions. Interestingly, there are no clear patterns of precipitation-related variables being correlated with the responses to the drought stress or temperature-related variables being correlated with the responses to the heat stress as might be expected. In fact, it almost seems the opposite, with more correlations between temperature-related variables and drought, and more correlations between precipitation-related variables and heat (Figure 11). Also, there are correlations between 13 climate variables and the combined heat and drought stress, compared with correlations between only six variables with either the drought alone or the heat alone. This underlines the complexity of climate and the close ties between temperature and precipitation and emphasizes why it is necessary to study abiotic stresses in combination.

Genome-wide association mapping found SNPs significantly associated with *B. distachyon* response to heat and drought stress conditions

A genome-wide association study was conducted to identify genetic loci associated with changes in plant phenotypes in response to heat and drought treatments. To assess the genetic basis of heat and drought responses in *B. distachyon* over time, GWAS was done using data from each of the four Time Points previously mentioned (Time Point 1 at 22 DAP, Time Point 2 at 28/29 DAP, Time Point 3 at 36/37 DAP, and Time Point 4 at 44/45 DAP – the final day with data for all treatments). Often, GWAS are done by using the measurement of the trait of interest under a stress condition, which can reveal associations between the genome and that trait under stress conditions. However, using the difference between a trait measurement under stress and control allows the GWAS to uncover associations between the genome and the *response* to the stress condition, which is the focus of this study. A separate GWAS was done for each stress treatment by taking the average of measurements for the specific trait of interest across all replicates for a given treatment at that time point, and taking the difference of those averages under the stresses compared to the average of the replicates under control conditions, and using this difference as the trait measurement for the GWAS (Bac-Molenaar et al., 2016; Davila Olivas et al., 2017; Gao et al., 2019). This was done for three phenotypic measurements: plant height, plant shoot area, and percent of shoot tissue damage. Full GWAS results are available in the Supporting Information (Data S4).

In total, 19 SNPs were significantly associated ($P <$ 1.71e-5) with either height or percent damage (Figure 12; Figures S5a, S6, Data S4). No SNPs were significantly associated with plant shoot area (Figure S5b, Data S4). The average linkage disequilibrium (LD) decay was found to be 100 000 bp at an $r^2 = 0.2$ (Figure S7., Data S5), a commonly used LD decay cutoff (Aoun et al., 2016; Gur et al., 2017), so candidate genes could be found within this range, upstream or downstream from a significant SNP. However, such a range can often contain hundreds of genes, and since this was a preliminary exploratory analysis of these genes, in this study only the two adjacent genes closest to a significant SNP were examined.

18 SNPs were significantly associated with height; 10 at Time Point 3 and eight at Time Point 4 (Figure 12). At Time Point 3, there were SNPs significantly associated with

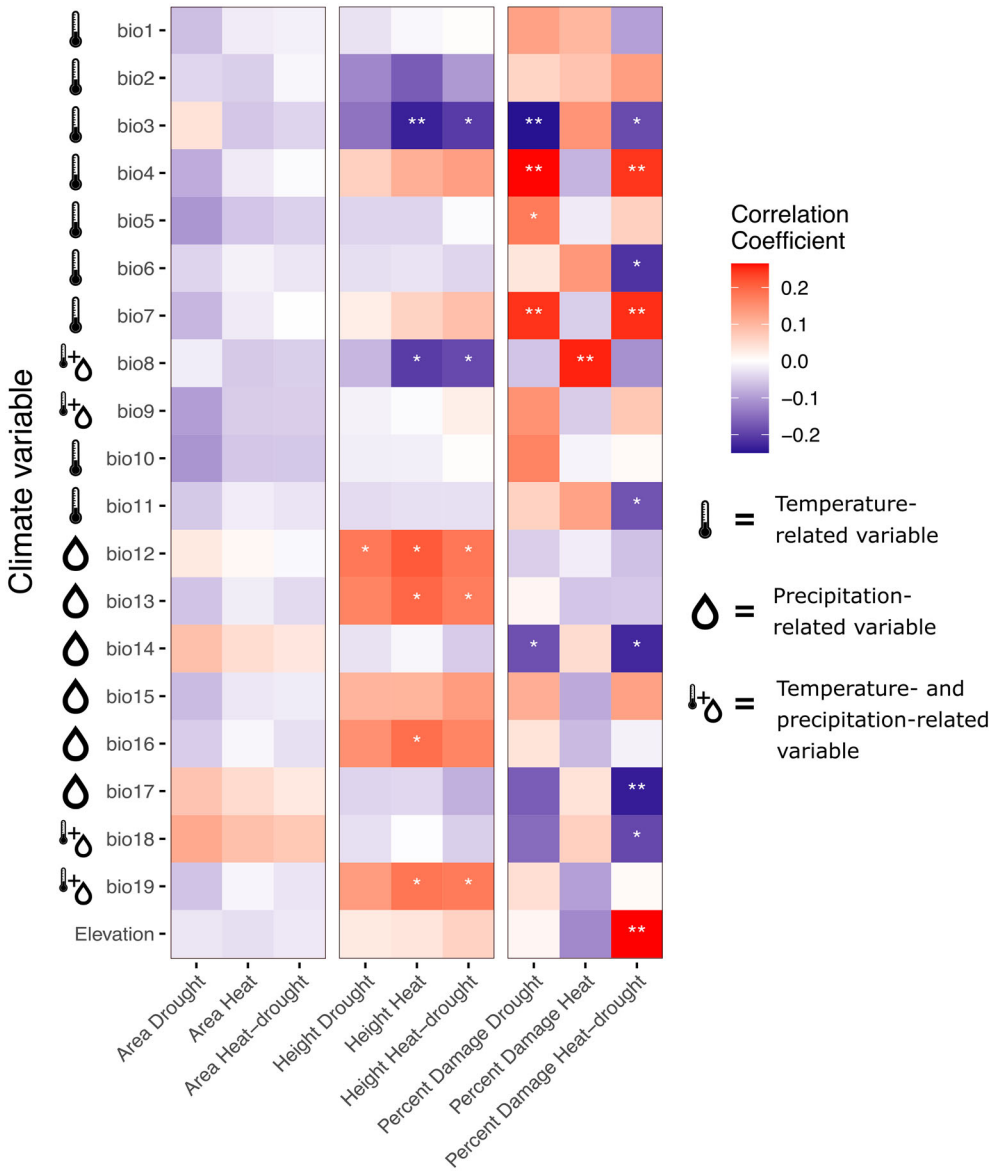

Figure 11. Heatmap of correlations between bioclimatic variables and plant responses to stress treatmentsHeatmap of correlations between the 19 bioclimatic variables from WorldClim plus elevation for each accession's climate of origin and changes in plant area, height, and percent damage in the stress treatments compared to control. Trait and treatment combinations are on the *x*-axis, and climate variables are on the *y*-axis. Symbols indicate the category of climatic variables. Bioclimatic variables variables are: bio1-annual mean temperature; bio2-mean diurnal range (mean of monthly max temp – min temp); bio3-isothermality (bio2/bio7)(×100); bio4-temperature seasonality (standard deviation × 100); bio5-max temperature of warmest month; bio6-min temperature of coldest month; bio7-temperature annual range (bio5-bio6); bio8-mean temperature of wettest quarter; bio9-mean temperature of driest quarter; bio10-mean temperature of warmest quarter; bio11-mean temperature of coldest quarter; bio12-annual precipitation; bio13-precipitation of wettest month; bio14-precipitation of driest month; bio15-precipitation seasonality (coefficient of variation); bio16-precipitation of wettest quarter; bio17-precipitation of driest quarter; bio18-precipitation of warmest quarter; bio19-precipitation of coldest quarter. Red indicates a positive correlation and blue indicates a negative correlation, with darker colors indicating a stronger correlation between a climate variable and a trait in a specific stress treatment, and lighter colors a weaker correlation. Significant correlations are denoted as follows: * $P < 0.05$, ** $P < 0.01$.

height in all three stress treatments, with one SNP, 123896_58 on chromosome 3, overlapping between the drought and heat treatments (Figure 12). At Time Point 4, SNPs were significantly associated with height in the heat and heat-drought treatments, with one SNP, 148978_31 on chromosome 4, overlapping between both of these stresses (Figure 12). Overall there was not much overlap from one time point to the next, but one SNP, 100003_43 on chromosome 3, was significantly associated with height in the drought treatment at Time Point 3, and in the heat treatment at Time Point 4. Only one SNP was significantly associated with percent damage, and this was at Time Point 4 in the heat treatment (Figure S5a).

A table of genes closest to SNPs that are significantly associated with plant height or percent damaged tissue is

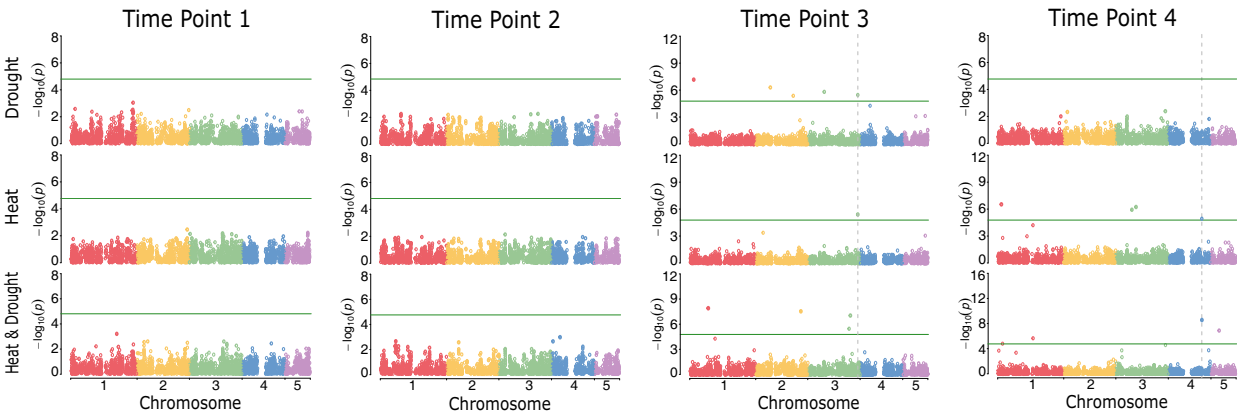

Figure 12. Manhattan plot of GWAS for plant height throughout the experimentsManhattan plot of GWAS results for height (difference between plant height in stress treatment and in control) at four time points throughout the experiments. Time Point 1 is 22 days after planting (DAP), Time Point 2 is 28/29 DAP, Time Point 3 is 36/37 DAP, and Time Point 4 is 44/45 DAP. Each point represents a SNP. The height of the SNP on the *y*-axis represents the strength of association with plant height, expressed as −log10(*P*-value). Points are colored by chromosome. The green horizontal line represents the significance cutoff and is calculated by dividing 0.05 by the number of SNPs included in the GWAS: $-log_{10}\left(\frac{0.05}{2,977}\right) = 4.7748$. Vertical dashed gray line indicates that an SNP is significantly associated with plant height in more than one stress treatment.

available in the Supporting Information (Data S6). These genes closest to significant SNPs are discussed further in the Discussion section and are potential targets to alter plant response to abiotic stress conditions.

DISCUSSION

Current elite crops have been bred to be extremely high-performing but not necessarily very tolerant to fluctuations in climate or weather patterns that expose crops to abiotic stresses (Mickelbart et al., 2015). Accordingly, it is valuable to explore the natural variation of phenotypes in weedy relatives to these major crops, to exploit their diversity in stress tolerance and improve that of current elite crops (Mickelbart et al., 2015). *B. distachyon* is an example of a weedy relative of major food and biofuel crops with natural phenotypic variation (International Brachypodium Initiative, 2010). Studying this powerful model of C_3 grass to assess its natural variation and understand genetic loci associated with its abiotic stress responses could aid in improving abiotic stress tolerance in the elite crops that feed and fuel the world's growing population. Also, the anticipated increase in drought and heat stresses as a result of climate change and the distinct impact of stresses in combination underscores the importance of phenotyping plants under multiple stresses that frequently co-occur.

The differences in responses to individual versus combined abiotic stresses are central to this study. For plant biomass accumulation (plant shoot area and height), the combination of heat and drought stress is generally the most detrimental for *B. distachyon* (Figure 6; Figure S2). *B. distachyon* accessions accumulated less biomass in the combination of stress conditions compared to when exposed to heat or drought stresses individually (Figure 6; Figure S2). Plants in heat stress were also much smaller than in drought stress and closer in size to plants in the heat and drought combination, but on average were still larger than in the combination stress treatment (Figure 6; Figure S2). These results alone might indicate that the combination of heat and drought stresses is more severe than individual stresses. However, when considering all results of this study, particularly tissue damage, *B. distachyon* responses to heat stress seem to be more detrimental than those to the drought treatment applied or the combination of these two stresses for *B. distachyon*. Further, when comparing all measured phenotypes in this study, the drought stress is distinct from both heat-related stresses, since more overlap in responses was observed between the heat and heat-drought stresses (Figure 3). Variance in phenotype explained by genotype, treatment, and the genotype-treatment interaction shows the treatment effect appearing earlier for the heat and heat-drought treatments compared to the drought treatment (Figure 8). The treatment effect is also larger for most traits in both heat-related treatments than in the drought treatment (Figure 8), suggesting that the heat treatments may have a stronger effect than the drought treatment in this study.

Fitting with the variance explained data, estimated plant tissue damage in *B. distachyon* was generally the highest in response to heat stress alone, in comparison to either drought alone or the combination of heat and drought (Figure 4). This could, in part, be affected by the control and drought treatments being done in one experiment, and heat and the combined heat drought in another. However, both the heat and heat-drought treatments were conducted in the same experiment, so they can be directly compared, and plants in the heat treatment overall had

much more damage than those in the combined stress, which was a very unexpected result. Also, considering that at the beginning of both experiments, there were no major differences between the plants in the different experiments (Figure 3), the magnitude of the difference in percent damage in the heat treatment compared to drought is so large (more than double), it seems highly unlikely that this is only caused by differences between the two highly controlled experiments.

Overall, though past studies suggest that the responses to the combination of drought and heat stress would generally be more severe than individual stresses (Atkinson et al., 2013; Balfagón et al., 2020; Choudhury et al., 2017; Mittler, 2006; Rasmussen et al., 2013; Rizhsky et al., 2002, 2004), our data show that, when taking the plant tissue damage trait into account, heat stress caused the most detrimental response in *B. distachyon* under the tested conditions. These results suggest that *B. distachyon* may have stress avoidance strategies to survive hot and dry conditions by slowing growth and accumulating less biomass under drought stress and the combined heat and drought stress, while still maintaining healthy tissue. Although *B. distachyon* can accumulate marginally more biomass in heat than in the combination of heat and drought, the high amount of estimated tissue damage suggests that *B. distachyon* is not well-equipped to survive under heat and well-watered conditions.

As previously mentioned, abiotic stresses like heat and drought are often found to occur simultaneously in nature, so it is possible that *B. distachyon* has adapted to maintain healthy tissue under a combination of drought and heat but not under heat alone. In fact, the native growth region of *B. distachyon* is in the Mediterranean and Middle East, regions of the world that are generally warm or hot and very arid (Draper et al., 2001; Filiz et al., 2009; Garvin et al., 2008). According to the most recent Köppen–Geiger climate classification, the collection locations of the *B. distachyon* accessions examined in this study are generally classified as arid or temperate, with dry summers (Peel & Mahon, 2007). This is corroborated by the climate data presented from WorldClim, which shows that the climates of origin of these *B. distachyon* accessions are hot and dry, or cool and wet, in different seasons (Figure S4), and overall receive relatively low amounts of precipitation annually. This region is warm and typically does not receive much precipitation, so *B. distachyon* would likely very rarely be exposed to hot but well-watered conditions in its climates of origin. Consequently, it may be that when *B. distachyon* experiences heat stress, it is adapted to encounter drought as well, and is therefore more susceptible to water stress when well-watered in heat. Conversely, it could also be that when *B. distachyon* is exposed to drought, as it often is in its native climates, it is also adapted for heat stress, so when well-watered it is not prepared to maintain healthy tissue in heat. In this study, the heat and drought treatments began on the same day for the plants experiencing the combined heat and drought stress, however, the heat stress takes effect earlier, since the temperature increased within the span of a few hours, while it took days for the pots to dry down and the plants to begin experiencing the effects of the water-limitation. Therefore, it seems reasonable to hypothesize that for the plants in the combined stress treatment group, the heat primed them for drought, which is why they were able to maintain healthy shoot tissue throughout the experiment, in contrast to the plants in the heat only treatment group, which were also primed to experience drought but were then well-watered. This could be due to differences in transpiration or water use efficiency in response to the individual and combined stresses, which is an important avenue to explore in future studies to help elucidate the mechanisms by which *B. distachyon* responds to different stresses and their combinations.

While the climates of origin of these *B. distachyon* accessions have similarities – generally dry and warm or hot summers with cooler, wetter winters – the climate data from WorldClim presented also show variation in these climates of origin (Figure 10). Analyses of these climate data and *B. distachyon* phenotype under drought and heat stresses revealed significant associations between the climate of origin and *B. distachyon* responses to these stresses. This suggests that these accessions may be locally adapted to their climate of origin, which is driving their responses to these heat and drought stresses. Two accessions, BdTR10E and BdTR5J, illustrate this possibility. Both accessions are from Turkey, but from different geographic regions with distinct climates, and have contrasting responses to the drought and heat stresses in this study. BdTR10E was one of the accessions identified as being *most* tolerant to all three stress treatments, compared to BdTR5J, which was identified as being one of the *least* tolerant to these stresses (Figure 7; Data S2). BdTR10E is from the Southeastern Anatolia Region of Turkey (Filiz et al., 2009), which is a relatively low-lying area of the country (Figure 1; Data S1). The collection location of BdTR10E sits at an elevation of 448 m above sea level and has a hot and dry climate with low amounts of precipitation (Data S1). In contrast, BdTR5J is from the Central Anatolia Region of Turkey in the Köroğlu Mountains (Figure 1; Data S1) (Filiz et al., 2009). It was collected at an elevation of 1556 m above sea level, in a climate that is cooler overall, especially during the dry season and receives more precipitation, even during the warmer season (Data S1). These data show that BdTR10E was collected in an area with a much hotter and drier climate than where BdTR5J originates from. This is especially interesting considering that BdTR10E performed well under drought and heat stress conditions, and BdTR5J performed poorly under these

stress treatments (Figure 5). This could suggest that these accessions are locally adapted to their climates of origin. However, reciprocal transplant experiments would be required to test this hypothesis to see if there are higher rates of survival and fitness for *B. distachyon* accessions in their home environments.

As mentioned previously, a challenge in studying abiotic stress tolerance is the diverse ways in which these stresses can be experimentally applied, and that accessions are conflictingly described as tolerant or susceptible in different studies. The data presented in this study is no exception, as BdTR2C and Bis-1 were both identified as accessions displaying resilient growth in the drought stress applied (Data S2). However, both of these accessions were identified as drought susceptible in the 2011 study done by Luo et al. (Luo et al., 2011). Similarly, in this study, Bd21-3 and BdTR13E were found to be susceptible to drought (Data S2), while Luo et al. identified these accessions as moderately drought tolerant (Luo et al., 2011). Des Marais et al. assessed *B. distachyon* growth under similar conditions to this study – cool wet (control), cool dry (drought), hot wet (heat), and hot dry (heat and drought combined) – and found that accessions grew best in the hot wet conditions (Des Marais et al., 2017). Similar results were reported in studies from 2017 and 2019, in which Shaar-Moshe et al. assessed Bd21-3 under drought, heat, and combined heat and drought treatments, among others, and reported an increase in plant biomass in their heat treatment (Shaar-Moshe et al., 2017, 2019). Tconflictslict with the results presented in this study, where all plants in the heat treatment were much smaller than in the control treatment (Figures 5 and 6; Figure S2). The results for the drought and combination heat-drought treatments were generally similar between this study and Des Marais et al. and the two Shaar Moshe et al. studies, with biomass reduced in these two treatments compared to control (Figures 5 and 6; Figure S2) (Des Marais et al., 2017; Shaar-Moshe et al., 2017, 2019). These similarities and differences between results from different studies highlight the challenges in comparing abiotic stress studies, especially because the stress treatments were applied in distinct ways, at different stages of growth and for varying durations, and data were collected using a range of techniques. This does, however, indicate that the same or similar stresses can have contrasting effects at different stages in the *B. distachyon* life cycle, and shows the need for future research into the effects of abiotic stresses at different stages in plant vegetative and reproductive growth. These differences between results from different studies on the same stresses also highlight the need for platforms such as the phenotyping system used in this study. Traits like biomass have historically only been possible to measure destructively in a one time measurement, so it was impossible to get information about an individual plant over time. Measurements like height could at least be measured non-destructively, but it can be very time- and labor-intensive to measure many plants, and therefore not feasible to do frequently throughout an experiment spanning multiple weeks with many plants. There are also phenotypes such as plant health or greenness, which have generally been measured with scoring done by humans, which, as with height measurements, can be time- and labor-intensive, and also very subjective and therefore difficult to compare and reproduce. With image analysis, it is possible to measure these traits more accurately and precisely over the course of an entire experiment, and results can be more reproducible.

This study found 19 genetic loci significantly associated with changes in *B. distachyon* height and percent damage in response to the different abiotic stress treatments compared to control conditions (Figure 12, Figures S5a, S6, Data S4). These results could point to genes that regulate *B. distachyon*'s responses to drought, heat, and the combination of drought and heat. While two SNPs were found to be significantly associated with height in multiple stress treatments, most significant SNPs were distinct between the different stress treatments, which suggests that the individual stresses likely activate unique sets of stress pathways, but also that the combined stress may activate different pathways compared to each stress individually (Figure 12; Figure S5). This suggests that different genes are associated with the responses to the tested abiotic stresses. Since heat and drought often activate different mechanisms by which plants respond to stresses (Atkinson & Urwin, 2012; Mittler, 2006; Rizhsky et al., 2002, 2004), it would not be surprising to discover that different genes are involved in drought tolerance compared to heat tolerance, as well as the combination of these two stresses.

18 SNPs were significantly associated with height at different times during the experiment (Figure 12). Notable candidate genes located near these SNPs significantly associated with height that are known to be involved in plant abiotic stress responses include a sugar transporter (Gautam et al., 2019; Gupta & Kaur, 2005; Kaur et al., 2021; Saddhe et al., 2021), a Replication Factor-A protein (Chowdhury et al., 2021; Ishibashi et al., 2005; Nisa et al., 2019), an autophagy (ATG) protein (Bassham et al., 2006; Dokladny et al., 2013; Zhou et al., 2014), and a fasciclin 1 (FAS1) domain (Faik et al., 2006; MacMillan et al., 2010; Pinski et al., 2019; Seifert, 2018) (Data S6). A particularly interesting candidate gene, in this case, is the *FAS1* domain-containing protein, which is in close proximity to the SNP significantly associated with height in both heat and the heat-drought treatments at Time Point 4 (Figure 12; Data S6). Fasciclin domains are a cell adhesion domain that is found in insects, animals, bacteria, fungi, and algae, and is found as a large family of fasciclin-like arabinogalactan proteins (FLAs) in higher plants (Faik et al., 2006;

MacMillan et al., 2010). Some FLAs have been linked to secondary cell wall synthesis in Arabidopsis stems, and with wood formation in tree trunks and branches, which suggests a role in the development of plant stems, and research into this gene family has found that FAS domain FLAs contribute to stem strength in plants by regulating cellulose deposition and affecting the integrity of the cell-wall matrix (MacMillan et al., 2010). Studies have shown that FLA genes are involved in plant abiotic stress response, including findings showing that some FLA genes were up- or down-regulated in response to abiotic stress including heat and dehydration in wheat (*Triticum aestivum*) (Faik et al., 2006) and that rice (*Oryza sativa L.*) FLA genes also displayed differential expression patterns induced by abiotic stresses (Ma & Zhao, 2010). Besides close genetic relatives of *B. distachyon*, a study examining FLA transcript levels in response to temperature stress in *B. distachyon* found that multiple FLA genes were upregulated at high temperatures compared to the control (Pinski et al., 2019). This candidate gene is especially noteworthy considering the role that FLA genes play in cell wall development and stem strength in plants and that this SNP is significantly associated with height, which would be impacted by stem strength and development.

One SNP was significantly associated with the percent shoot damage in the heat stress condition (Figure S5a, Data S4). One notable candidate gene located near this SNP significantly associated with percent damage encodes a spindle- and kinetochore-associated (Ska) protein 2 (Data S6). Ska proteins form a complex with at least three parts, made of Ska1, Ska2, and Ska3, that are involved in cell division (Gaitanos et al., 2009; Hanisch et al., 2006; Helgeson et al., 2018). The Ska complex associates with the spindle and kinetochore during mitosis, and cells with reduced Ska levels had much longer delays before transitioning into anaphase from metaphase (Gaitanos et al., 2009; Hanisch et al., 2006). Not much is known about the involvement of the Ska complex in plant responses to abiotic stresses, but the kinetochore structure in human cells showed increased sensitivity to temperature stress in the absence of Ska1 and Ska2 (Hanisch et al., 2006), and plant Ska genes are homologous to those in animals (Yamada & Goshima, 2017).

This work found interesting correlations between the *B. distachyon* climate of origin and the responses to heat and drought stresses, which need to be explored further in future work. This study also identified potential causative loci for heat and drought responses in *B. distachyon* and contributes new sequencing data to the community. This dataset can be leveraged for future studies into uncovering the mechanism of heat and drought tolerance in *B. distachyon*, which may allow for genetic modifications or targeted breeding efforts to improve abiotic stress tolerance of current major food and biofuel crops.

EXPERIMENTAL PROCEDURES

Plant material

Diploid accessions of *B. distachyon* from the USDA and the Mur Lab (University of Aberystwyth) were used in both phenotyping experiments. The population of *B. distachyon* accessions used in this project was collected throughout this model plant's native range in the Mediterranean and the Middle East (Draper et al., 2001; Filiz et al., 2009; Garvin et al., 2008; Tyler et al., 2016). The majority of accessions were collected in Turkey and Spain, but the distribution of this population's collection locations can be seen in Figure 1. More detailed information regarding the collection locations of these accessions can be found in the Supporting Information (Data S1). 137 accessions were included in the experiment with drought and control conditions, and 144 accessions were used in the experiment with heat and heat-drought conditions. These were overlapping sets of *B. distachyon* accessions, with 132 being included in both experiments. Approximately 4 replicate plants of each accession were included for every treatment.

Plant growth and application of stress treatments

The *B. distachyon* accessions in each experiment were split into two groups and planted in plug trays on either day 1 or day 2 of both experiments (control and drought; heat and heat-drought). Splitting the accessions into two planting groups made it possible to compare plants of the same age in images taken throughout the experiment since plants were imaged every other day. Seeds were planted in plug trays and allowed to germinate for 3 days. After germinating, accessions were transplanted to prefilled pots and allowed to grow for 10 days in a Conviron growth chamber. The pots used were 4-inch diameter white/gray pots from Hummert, prefilled with ~473 ml of MetroMix360 soil premixed with 0.5 g of Osmocote Classic 14-14-14 fertilizer (Everris NA Inc., Dublin, OH, USA). After 10 days of growth, pots were barcoded, then returned to the Conviron growth chamber for an additional 2 days. Barcoded information included genotype identification, water treatment group, and a unique pot identification number. During the germination and pre-growth period for both experiments, plants were grown under a 14-h photoperiod (14 h day/10 h night) at 22°C day/18°C night, 50% relative humidity, and light intensity of ~200 μmol/m^2/sec. At 15 days after planting (DAP) the two groups of plants were loaded into the Conviron growth chamber of the Bellwether Phenotyping Platform.

In both experiments, plants were grown under 14 h-photoperiod (14 h day/10 h night) with a light intensity of 200 μmol/m^2/sec and relative humidity at 50% on the Bellwether Phenotyping Platform (Figure S1). In the control and drought experiment, the temperature was 22°C during the day and 18°C at night, and in the heat and heat-drought experiment it was 35°C during the day and 30°C at night (Figure S1). The water treatments were done by watering to a specific target weight for each treatment. These target weights were calculated by using the method described by Fahlgren et al. (2015). In short: pre-filled pots that had been completely dried down were weighed, then fully saturated with reverse osmosis water and weighed again after allowing the water to absorb. This was classified as being watered to 100% and was used as the target weight for the well-watered treatment. 20% of the water amount added to the 100% watering treatment was used for the water-limited (drought) treatment. For the first four days on the phenotyping platform, all plants (regardless of treatment) in both experiments were watered to 100%, with the 20% water-limited treatment being imposed on the plants in the drought and heat-drought treatment groups on the fifth day

on the platform. Plants were weighed three times daily and watered (or not watered) to a specific weight.

Image processing and extraction of trait information

RGB (red, green, blue) images of all individual plants were captured every other day in the Bellwether Phenotyping Facility at the Donald Danforth Plant Science Center (Fahlgren et al., 2015), acquiring side-view images from four angular rotations (0°, 90°, 180°, 270°). The RGB camera on this system is a ⅔″ progressive scan CCD camera (Basler AG, Ahrensburg, Germany) with an image resolution of 2454 × 2053 pixels. Due to the time it takes to image all plants on the phenotyping platform, only half of the plants could be imaged each day, so plants were imaged every other day. Plant growth was staggered to account for this. Half of the plants were assigned to be imaged on odd days, and the other half on even days. To ensure the entire plant was included in each image, the optical zoom was adjusted throughout the experiment as the plants grew in size. In the experiment with heat and heat-drought conditions, a power failure in the imaging system at 26 DAP caused imaging to be shifted by one day. For imaging after this point, the DAP with corresponding images were combined (26 and 27, 28 and 29, etc) to allow for comparison between the two experiments. The images taken in these experiments are publicly available on CyVerse at: https://datacommons.cyverse.org/browse/iplant/home/shared/danforth_center/Ludwig_et_al_Brachypodium.

Images were analyzed using the open-source image analysis software PlantCV (Gehan et al., 2017). PlantCV v3.8 (Fahlgren et al., 2020) was used to analyze each camera angle and zoom level. To segment the plant from background, the RGB image was converted to the HSV and LAB color spaces and the saturation and blue-yellow channels were isolated. Thresholds were applied to the saturation channel and the blue-yellow channels and the two binary images were combined. The fill function of PlantCV was used to fill in any noise (objects smaller than 50 pixels) that were left over after combining the two binary images. The cleaned binary image was used to mask the original RGB image so that the pot, carrier, and background were removed. A Region of Interest (ROI) was set around the plant to further isolate it from the background, and only objects that overlapped the ROI were kept for analysis. After segmentation of the target object (plant) from the background, morphological characteristics were extracted using the PlantCV 'analyze_object' function (Gehan et al., 2017). Additionally, the PlantCV naïve Bayes classifier module (Abbasi & Fahlgren, 2016; Gehan et al., 2017) was trained to label plant pixels as either 'healthy' or 'unhealthy" to determine what percentage of the plant in each image was stressed or damaged by its growth conditions. The training was done by choosing a representative set of 10 RGB images and using the Pixel Inspection Tool in ImageJ (Abràmoff et al., 2004) to gather color value training data for over 1000 pixels from each of three categories: healthy plant tissue, unhealthy plant tissue, and background. These classifications were based on color, with pixels chosen from green, healthy-looking plant tissue for the 'healthy" category, pixels from yellow or brown, unhealthy-looking plant tissue for the 'unhealthy' category, and non-plant pixels for the background. The pixel color data was then used in PlantCV to train the naïve Bayes classifier, which was included in the Python scripts run over each image to assign the plant pixels to the appropriate category of interest. The percentage of damaged tissue was calculated by dividing the shoot area classified as unhealthy by the total shoot area in R (R Core Team, 2020). Representative images of a few of the outputs from PlantCV, including the naïve Bayes classifier, used in the analysis of this data are shown in Figure S8.

To correct for the different zoom levels in the images, scaling factors for both height and area were calculated in R (R Core Team, 2020) using a reference object of known size as was done in Fahlgren et al. (2015). The dimensions of the known object were measured in centimeters and it was imaged with the same imaging setup and at the same zoom levels used in the *B. distachyon* phenotyping experiments. The height and area of the known object were then measured in pixels, which allowed a conversion factor to be calculated. This was used to convert pixel measurements from PlantCV to centimeters or centimeters squared, which allowed pixel heights and areas that represent plant phenotypes to be compared across zoom levels in downstream analysis. It has been well established in previous work that there is a strong correlation between the plant area calculated from images and manually measured fresh weight of aboveground biomass (Chen et al., 2014; Fahlgren et al., 2015; Honsdorf et al., 2014; Leister et al., 1999; Rajendran et al., 2009), and the data collected in this study are no exception. Fresh weight in grams was significantly positively correlated with plant area from PlantCV ($r = 0.98$; $P < 2.2 \times 10^{-16}$; Figure S9) on the final day of these experiments.

R analysis scripts and Python scripts for image analysis and trait extraction done with PlantCV, and all other analysis scripts and their required input files, are available in the public GitHub repository at this link: https://github.com/danforthcenter/brachypodium-heat-drought-paper.

High-resolution spatial climate data

The climate data used for the climate analysis in this study were obtained from WorldClim V.2.1, a long-term global climate dataset (Fick & Hijmans, 2017). WorldClim provides monthly high-resolution spatial gridded data of 19 bioclimatic variables for a 30-year reference period between 1970 and 2000 at a resolution of 30 arcseconds, which is approximately 1 km^2 on the Earth's surface (Fick & Hijmans, 2017). These data are interpolated using in situ observations at hydro-meteorological stations from various programs, data sources, and entities, including the global historical Climatology Network (ghCN), the World Meteorological Organization (WMO), and the International Center for Tropical Agriculture (ClaT), among others (Fick & Hijmans, 2017). The Euclidean distance between each accession's collection location and the WorldClim data points were calculated to find the closest available climate data for each accession's climate of origin. Climate data from WorldClim was adequately close (Euclidean distance $< \sqrt{2}$km) to 147 out of the total 149 accessions examined in this study (Data S1). These climate data were used to conduct a PCA in R.

Low-Coverage sequencing

Plant tissue was collected from each accession following the completion of the phenotyping experiments. Genomic DNA was extracted using a Qiagen DNeasy 96 Plant kit (catalog number: 69181) and quantified using a Qubit dsDNA HS Assay Kit (catalog number: Q32851) and Qubit 2.0 Fluorometer (Life Technologies, Carlsbad,CA, USA). 200 ng of DNA for each accession were aliquoted in two 96-well plates and GBS libraries were constructed using the protocol described in Huang et al. (Huang et al., 2014) with *Pst*I-HF and *Msp*I restriction enzymes for 145 accessions of *B. distachyon* used in this study. These libraries were sequenced by the Genome Technology Access Center at Washington University in St. Louis. GBS data for this population of *B. distachyon* is available at the Short Read Archive (SRA) PRJNA312869.

SNP calling and population structure estimation

To call SNPs (single-nucleotide polymorphisms) from the GBS data collected in this experiment, the Burrows–Wheeler Aligner (BWA) was first used to align all accession genomes to the *B. distachyon* reference genome (Li, 2013). BWA version 0.7.12-r1039 was used (Li, 2013). The most commonly used reference accession for *B. distachyon* is Bd21-0, and the newest genome assembly and annotation for this accession (version 3.2 from 2020) that can be found on Phytozome was used for alignment (Goodstein et al., 2012; Haas et al., 2003; Salamov & Solovyev, 2000; Smit et al., 1996-2010; Yeh et al., 2001). Next, the SAMtools version 1.11 view function was used to convert the SAM (Sequence Alignment/Map) files output by BWA to BAM (Binary Alignment Map) files, which are the binary equivalent of a SAM file (Danecek et al., 2021). The BAM files were then sorted using the sort function from SAMtools, which sorts genome alignments by leftmost coordinates (Danecek et al., 2021). These sorted BAM files were then used in 'gstacks', a Stacks program (Catchen et al., 2011, 2013), in the reference-based mode, to call SNPs at each locus relative to the reference genome, and genotype each individual at every SNP identified (Catchen et al., 2011, 2013). Gstacks then phased these SNPs into a set of haplotypes for each individual at every locus (Catchen et al., 2011, 2013). SNPs called by gstacks and a population map were then input into 'populations', another Stacks program, to compute population genetics statistics (Catchen et al., 2011, 2013). In 'populations', options used included -t set to 10 to use 10 threads, –r set to 0.8 to set the minimum percentage of individuals in the population required to process the locus, –min-maf set to 0.05 to filter SNPs with a minor allele frequency less than 0.05, –write-single-snp to restrict data analysis to only the first SNP per locus, –plink to output genotypes in PLINK format, –structure to output results in Structure format, and –vcf to output SNPs and haplotypes in Variant Call Format ('vcf") (Catchen et al., 2011, 2013). Stacks version 2.4 was used for both 'gstacks' and 'populations' (Catchen et al., 2011, 2013). After this, PLINK v1.90b6.21 was used to do a principal component analysis (PCA) on the output from populations, to find the population structure of *B. distachyon* based on samples in this study (Chang et al., 2015; Purcell et al., 2007). The –allow-extra-chr option was used in addition to default parameters for the PLINK –pca function, to allow the *B. distachyon* chromosome codes to be read (Chang et al., 2015; Purcell et al., 2007).

Based on the clustering in the PCA to estimate population structure, the *B. distachyon* population in this study was divided into two main subpopulations (with some accessions falling outside these two main clusters). Using vcftools, the fixation index (Fst) values between these subpopulations were obtained (Danecek et al., 2011). Fst is a measure of the genetic variance contained in a subpopulation (the S subscript) relative to the total genetic variance (the T subscript) in a population-based on Wright's F-statistics (Wright, 1965). An Fst value of 0 indicates no genetic differentiation between the subpopulations, while an Fst value of 1 indicates complete differentiation (Bird et al., 2017; Holsinger & Weir, 2009). vcftools v0.1.14 was used with the option –weir-fst-pop to calculate Fst estimates based on Weir & Cockerham's, 1984 paper (Danecek et al., 2011; Weir & Cockerham, 1984). Scripts are available at (https://github.com/danforthcenter/brachypodium-heat-drought-paper).

Linkage disequilibrium decay estimation

The SNP catalog file in Variant Call Format ('vcf') was first sorted and converted into bed format using Plink v1.90b6.17, and pairwise linkage decay between markers on the same chromosome was calculated (Chang et al., 2015; Purcell et al., 2007). Following this, a bash script was used to extract the distances between the SNPs and the corresponding r^2 values. Using R, SNPs were categorized into bins of 10 kbps, and means were calculated per bin to estimate linkage disequilibrium decay for this population of *B. distachyon*. Scripts are available in the public GitHub repository (https://github.com/danforthcenter/brachypodium-heat-drought-paper).

Subselection of accessions used in data analysis

There were 137 *B. distachyon* accessions included in the experiment with drought and control conditions, and 144 were included in the experiment with heat and heat-drought conditions. Due to differences in germination and seed availability, 132 accessions were overlapping between both experiments, while the total number of *B. distachyon* accessions examined in either experiment is 149. The 132 accessions overlapping between the two experiments were used in analyses requiring direct comparisons between different treatments. For any analyses using the WorldClim climate data, only accessions with climate data available were used, which were 147 out of 149 included in the phenotyping experiments. In all other analyses, including the GWAS, many accessions that had complete data were included.

Statistical analysis on extracted trait information

All statistical analyses were done in R, using R version 4.0.1 (released June 6, 2020) (R Core Team, 2020). Additional packages used include corrplot (Wei & Simko, 2017), and data.table (Dowle & Srinivasan, 2020), dplyr (Wickham et al., 2021), factoextra (Kassambara & Mundt, 2020), FactoMineR (Lê et al., 2008), GAPIT (Wang & Zhang, 2021), ggplot2 (Wickham, 2016), gplots (Warnes et al., 2020), lme4 (Bates et al., 2015), plyr (Wickham, 2011), raster (Hijmans, 2020), readr (Wickham et al., 2022), reshape2 (Wickham, 2007), tidyr (Wickham, 2020), and WorldClimTiles (kapitzas, 2020).

A random effects model (or variance components model) was used to calculate the variance explained by genotype, treatment, and the genotype-treatment interaction in plant traits. The model was fitted using the lmer function from the lme4 package in R (Bates et al., 2015). In this model, a type 3 sum of squares was measured for each plant trait. Those terms were normalized to display a percentage of each plant trait's total variance explained by the design variables and their interactions.

The GWAS in this study was conducted by using the FarmCPU method implemented in GAPIT Version 3 in R (Liu et al., 2016; Wang & Zhang, 2021). Past studies have established that *B. distachyon* has a very strong population structure (Draper et al., 2001; Filiz et al., 2009; Garvin et al., 2008; Tyler et al., 2016), which was also seen in this study, so the FarmCPU method was used to eliminate false positives due to population structure (Liu et al., 2016). This method also can include additional covariates to account for population structure or other associations that could lead to false positive results (Liu et al., 2016). Therefore, FarmCPU was first run with 'Model.selection = TRUE' so that forward model selection using the Bayesian information criterion (BIC) was conducted to determine the appropriate number of covariates included in the GWAS model (Wang & Zhang, 2021). For all phenotype and treatment combinations, the optimal model included zero covariates for both population structure and climate based on the BIC values, so all FarmCPU runs were done without any manually supplied covariates. A kinship matrix was created with GAPIT using the default 'VanRaden' method to show genetic relatedness of these *B. distachyon* accessions (Figure S3) (VanRaden, 2008; Wang & Zhang, 2021).

The inputs required to run GAPIT include a genotype file and a phenotype file (Wang & Zhang, 2021). In this case, the phenotype file was created using the data output from PlantCV for three traits: plant height, plant shoot area (to approximate biomass), and the percent damage (to approximate plant stress). To create this file, the average was found for all images taken of each accession at the chosen time point for a given trait, and then the difference between the average of the trait in the stress treatment and the average under control conditions was used as the phenotype value for that accession. This removes the genotype effect and ensures that the ensuing results are due to the treatment effect (GxE). A HapMap file was created by using TASSEL v5.0 (Bradbury et al., 2007) to convert the file containing the genotype and SNP information in variant call format (VCF) to HapMap format using a custom HTCondor job file to input as the genotype file in GAPIT. Since TASSEL requires the VCF file to be sorted by the position column before it can be loaded and used, this sorting was done by using the SortGenotypeFilePlugin in TASSEL v5.0 (Bradbury et al., 2007), also with a custom HTCondor job file. Since there was no complete overlap in the accessions used in the two experiments and there were a few accessions that did not have complete data at each time point in a particular treatment, not all accessions could be included in the GWAS. For each time point, all accessions that had genotype information and trait data for each treatment were used (GWAS input files are available in the public GitHub repository).

GAPIT was run with default options, with the addition of the 'Multiple_analyses = TRUE' option to output combined Manhattan plots and quantile-quantile (Q-Q) plots for each run (Wang & Zhang, 2021). All other outputs are standard from GAPIT.

The GWAS results were analyzed using ZBrowse (Ziegler et al., 2015), an interactive GWAS viewer that runs on R (R Core Team, 2020). The GWAS results from GAPIT were uploaded to ZBrowse and aligned to the most recent *B. distachyon* reference genome (version 3.2 from 2020) from Phytozome (Goodstein et al., 2012). The two genes closest to each significant SNP (one upstream and one downstream) from each GWAS were examined.

For more detail about the data analysis, scripts for all analyses done in R are provided in a public GitHub repository (https://github.com/danforthcenter/brachypodium-heat-drought-paper).

ACKNOWLEDGEMENTS

We would like to acknowledge the tremendous loss of Dr. Todd C. Mockler, who passed away while this paper was in final preparation, to the Brachypodium Community and to the genomics and phenomics communities at large. This work started in Dr. Mockler's lab and many authors on this paper were mentored by him. We would like to thank Kevin Reilly and his team for growth chamber and greenhouse plant care and support. We would also like to thank Melinda Darnell for expert care of the Bellwether Phenotyping Platform during the course of these experiments, to the Bellwether Foundation for the generous donation that allowed for the construction of the Bellwether Phenotyping Platform (RRID: SCR_019049), and DDPSC Facilities for careful maintenance of the Bellwether Platform.

AUTHOR CONTRIBUTIONS

MAG, EL, and TCM conceived the research; MAG designed the experiments; MAG and NF developed tools for the experiments; EA, KH, KG, MAG, and TF did the experiments; EL, MAG, JB, NF, SP, and JS analyzed images and data; EL and MAG wrote the article; EL, JB, JS, KG, MAG, and NF edited the article.

FUNDING

This work was supported by the National Science Foundation (IOS-1202682 and 1921724 to M.A.G.), the United States Department of Energy (DE-SC0006627 to T.C.M), the United States Department of Agriculture – National Institute of Food and Agriculture (2019–67021-29926 and 2022-67021-36467 to M.A.G. and N.F.) and the Donald Danforth Plant Science Center.

CONFLICT OF INTEREST STATEMENT

The authors declare that they have no conflicts of interest.

SUPPORTING INFORMATION

Additional Supporting Information may be found in the online version of this article.

Figure S1. Daily temperature, percent relative humidity, and light intensity measurements from the growth chamber in the phenotyping platform

Plots of measurements taken by sensors inside the Conviron growth chamber that is part of the Bellwether Phenotyping Platform where the plants in this study were grown throughout both experiments. In the first column are measurements for daily temperature, percent relative humidity, and light intensity from the experiment at control temperatures, which included the control and drought treatments. In the second column are measurements for daily temperature, percent relative humidity, and light intensity from the experiment at high temperatures which included the heat and heat-drought treatments. The two sets of lines in the daily temperature plot in this column represent the time before (dark blue) and after (light blue) the temperature was raised to begin the heat treatment after 5 days on the system. Other deviations from the setpoint for temperature, relative humidity, and light intensity in this experiment are due to a brief power failure of the system during the experiment.

Figure S2. Heatmaps of plant area throughout the experiments. Heatmaps of average plant area in the four experimental conditions (from left to right: control, drought, heat, heat, and drought combined). This was calculated by taking the mean area of all plants of the same accession in the same treatment on each day they were imaged. The *x*-axis of each heatmap shows days after planting (DAP). On the *y*-axis are the accessions, sorted alphabetically in descending order. White boxes indicate missing data. Common color key for all treatments in the top left; orange indicates smaller plants, and blue indicates larger plants.

Figure S3. Heatmap and dendrogram of kinship matrix for the *B. distachyon* accessions assessed. A heatmap and dendrogram of kinship matrix illustrating the genetic relationship between 144 of the 149 accessions of *B. distachyon* assessed in this study. Created with GAPIT (Wang & Zhang, 2021), using the default 'VanRaden' method (VanRaden, 2008), based on 2977 high-quality SNPs with MAF >5%. The histogram in the color key represents the number of coefficient values within a corresponding color bar. X- and y-axes are colored by the country of origin of these accessions.

Figure S4. Correlation plot of bioclimatic variables. The correlation between variables used in the PCA of climates of origin. The climate data point from WorldClim that was closest to each accession's collection location was used as its climate of origin. Larger, darker circles represent stronger correlations between variables

and smaller, lighter circles represent weaker correlations between variables. The plot is ordered by 'first principal component order' (FPC) and was created with the corrplot package in R (Wei & Simko, 2017).

Figure S5. Manhattan plot of GWAS for percent damage and plant area throughout the experiments. Manhattan plot of GWAS results for the change in (a) percent damage (b) and plant shoot area under stress treatment in comparison to control conditions at four time points throughout the experiments. Time Point 1 is 22 days after planting (DAP), Time Point 2 is 28/29 DAP, Time Point 3 is 36/37 DAP, and Time Point 4 is 44/45 DAP. Each point represents a SNP. The height of the SNP on the *y*-axis represents the strength of association with (a) percent damage or (b) plant area, expressed as −log10(*P*-value). Points are colored by chromosome. The green horizontal line represents the significance cutoff and is calculated by dividing 0.05 by the number of SNPs included in the GWAS: $-log_{10}\left(\frac{0.05}{2,977}\right) = 4.7748$.

Figure S6. Quantile-quantile (Q-Q) plots for GWAS of plant height, plant area, percent damage. Q-Q plots showing the comparison of GWAS p-values for each SNP (*y*-axis) plotted against predicted p-values based on a normal distribution (*x*-axis) for (a) height, (b) area, and (c) percent damage. Time Point 1 is 22 days after planting (DAP), Time Point 2 is 28/29 DAP, Time Point 3 is 36/37 DAP, and Time Point 4 is 44/45 DAP. The areas shaded in gray indicate the 95% confidence interval. Each point represents an SNP and is colored by treatment.

Figure S7. Plot of genome-wide linkage disequilibrium (LD) decay. Plot representing genome-wide linkage disequilibrium (LD) decay for this *B. distachyon* population based on 2977 high-quality single nucleotide polymorphisms (SNPs). The *x*-axis represents the distance apart in base pairs (bp), and the *y*-axis is LD, based on the r^2 value. Points represent the LD between pairs of SNPs, and the line plots the average LD.

Figure S8. Example of input and output images from PlantCV. Representative input and output images from PlantCV. (a) Example of a side-view image captured during the experiments that would be used as an input for the PlantCV image-analysis pipeline. (b) Example of the 'height_above_reference' output from PlantCV. This measurement was used as the plant height. (c) Example of the 'area' output from PlantCV. (d/e) Example of the naïve Bayes classifier categorizing plant pixels as either healthy (blue) in panel d or unhealthy (orange) in panel e, which was used to find the percentage of damaged tissue for each plant.

Figure S9. Correlation between PlantCV-calculated plant area and manually measured plant fresh weight. Plant area calculated with PlantCV compared with manually measured fresh weight at the end of the experiment. The *x*-axis is measured fresh weight in grams, the *y*-axis is plant area from PlantCV in cm^2. Points are all plants in the two phenotyping experiments. A regression line with $R = 0.98$, $P < 2.2 \times 10^{-16}$, and standard error is plotted.

Data S1. Table of data from climate of origin

Table of all 149 accessions included in this study with collection location and climate of origin data. Collection location information (Country, Longitude, Latitude, Elevation) from original collectors (Draper et al., 2001; Filiz et al., 2009; Garvin et al., 2008; Tyler et al., 2016), and climate data from WorldClim v2.1 (Fick & Hijmans, 2017). The climate data point from WorldClim that was closest to each accession's collection location was used as its climate of origin.

Data S2. Tables of accessions ranked by performance in stress treatments. Tables of accessions ranked in descending order of performance in each treatment for the three main phenotypes assessed (area, height, percent damage). The difference between the traits in the stress treatments and control are included, as well as the normalized values (z-scores) of these differences. The ranking is based on the final column in each table 'mean_z', which is the mean of the z-scores for the accessions' responses to each treatment.

Data S3. Tables of values for percent variance explained by genotype, treatment, and genotype-treatment interaction at each time point. Tables of the variance explained between all stress treatments compared to control conditions. Includes variance explained by genotype, treatment, interaction (between genotype and treatment), and unexplained variance, by shape (PlantCV trait). Organized by time point (Time Point 1 is 22 days after planting (DAP), Time Point 2 is 28/29 DAP, Time Point 3 is 36/37 DAP, Time Point 4 is 44/45 DAP), and stress treatment.

Data S4. Tables of full results from GWAS for area, height, and percent damage. Tables of results from GAPIT (Wang & Zhang, 2021) for the GWAS done for area, height, and percent damage at all four time points were used to make Manhattan plots to visualize GWAS results. Time Point 1 is 22 days after planting (DAP), Time Point 2 is 28/29 DAP, Time Point 3 is 36/37 DAP, and Time Point 4 is 44/45 DAP.

Data S5. Table of linkage disequilibrium (LD) decay values. Table of genome-wide linkage disequilibrium (LD) decay values calculated using genotype-by-sequencing (GBS) data for 144 of the 149 accessions of *B. distachyon* assessed in this study (missing GBS data for the five accessions not included). This included 2977 high-quality single nucleotide polymorphisms (SNPs).

Data S6. Table of SNPs found to be significantly associated with *B. distachyon* height, area, or percent damage under stress conditions. Table of SNPs found by GWAS to be significantly associated with height, area, or percent damage with information about genes close to these SNPs. Includes information about SNPs, genes closest to SNP on either side, and the potential function of these genes.

OPEN RESEARCH BADGES

This article has earned an Open Materials badge for making publicly available the components of the research methodology needed to reproduce the reported procedure and analysis. All materials are available.

DATA AVAILABILITY STATEMENT

All raw and processed data have been made publicly available. Images from the two phenotyping experiments are available on CyVerse, sequencing data are available at the Short Read Archive (SRA) PRJNA312869, and all other data are available at the Github repository. Software used in this study is open-source or available for free. All links are in the Experimental Procedures section as well.

REFERENCES

Abbasi, A. & **Fahlgren, N.** (2016) Naïve Bayes pixel-level plant segmentation. In: *2016 IEEE Western New York image and signal processing workshop (WNYISPW)*. Rochester, NY: IEEE Xplore, pp. 1–4. Available from: https://doi.org/10.1109/WNYIPW.2016.7904790

Abràmoff, M.D., **Magalhães, P.J.** & **Ram, S.J.** (2004) Image processing with ImageJ. *Biophotonics International*, **11**, 36–42. Available from: https://dspace.library.uu.nl/handle/1874/204900

Allakhverdiev, S.I., **Kreslavski, V.D.**, **Klimov, V.V.**, **Los, D.A.**, **Carpentier, R.** & **Mohanty, P.** (2008) Heat stress: an overview of molecular responses in photosynthesis. *Photosynthesis Research*, **98**, 541–550. Available from: https://doi.org/10.1007/s11120-008-9331-0

Anderson, J.P., **Badruzsaufari, E.**, **Schenk, P.M.**, **Manners, J.M.**, **Desmond, O.J.**, **Ehlert, C.** ***et al.*** (2004) Antagonistic interaction between abscisic acid and jasmonate-ethylene signaling pathways modulates defense gene expression and disease resistance in Arabidopsis. *Plant Cell*, **16**, 3460–3479. Available from: http://www.plantcell.org/content/16/12/3460.short

Anderson, J.T., **Willis, J.H.** & **Mitchell-Olds, T.** (2011) Evolutionary genetics of plant adaptation. *Trends in Genetics*, **27**, 258–266. Available from: https://doi.org/10.1016/j.tig.2011.04.001

Aoun, M., **Breiland, M.**, **Kathryn Turner, M.**, **Loladze, A.**, **Chao, S.**, **Xu, S.S.** ***et al.*** (2016) Genome-wide association mapping of leaf rust response in a durum wheat worldwide germplasm collection. *Plant Genome*, **9**, 8. Available from: https://doi.org/10.3835/plantgenome2016.01.0008

Asselbergh, B., **De Vleesschauwer, D.** & **Höfte, M.** (2008) Global switches and fine-tuning—ABA modulates plant pathogen defense. *Molecular Plant-Microbe Interactions*, **21**, 709–719. Available from: https://doi.org/10.1094/MPMI-21-6-0709

Atkinson, N.J., **Lilley, C.J.** & **Urwin, P.E.** (2013) Identification of genes involved in the response of Arabidopsis to simultaneous biotic and abiotic stresses. *Plant Physiology*, **162**, 2028–2041. Available from: https://doi.org/10.1104/pp.113.222372

Atkinson, N.J. & **Urwin, P.E.** (2012) The interaction of plant biotic and abiotic stresses: from genes to the field. *Journal of Experimental Botany*, **63**, 3523–3543. Available from: https://doi.org/10.1093/jxb/ers100

Bac-Molenaar, J.A., **Granier, C.**, **Keurentjes, J.J.B.** & **Vreugdenhil, D.** (2016) Genome-wide association mapping of time-dependent growth responses to moderate drought stress in Arabidopsis. *Plant, Cell & Environment*, **39**, 88–102. Available from: https://doi.org/10.1111/pce.12595

Balfagón, D., **Zandalinas, S.I.**, **Mittler, R.** & **Gómez-Cadenas, A.** (2020) High temperatures modify plant responses to abiotic stress conditions. *Physiologia Plantarum*, **170**, 335–344. Available from: https://doi.org/10.1111/ppl.13151

Bassham, D.C., **Laporte, M.**, **Marty, F.**, **Moriyasu, Y.**, **Ohsumi, Y.**, **Olsen, L.J.** ***et al.*** (2006) Autophagy in development and stress responses of plants. *Autophagy*, **2**, 2–11. Available from: https://doi.org/10.4161/auto.2092

Bates, D., **Mächler, M.**, **Bolker, B.** & **Walker, S.** (2015) Fitting linear mixed-effects models using lme4. *Journal of Statistical Software*, **67**, 1–48. Available from: https://doi.org/10.18637/jss.v067.i01

Benavente, E., **García-Toledano, L.**, **Carrillo, J.M.** & **Quemada, M.** (2013) Thermographic imaging: assessment of drought and heat tolerance in Spanish germplasm of Brachypodium distachyon. *Procedia Environmental Sciences*, **19**, 262–266. Available from: https://linkinghub.elsevier.com/retrieve/pii/S1878029613003009

Bird, K.A., **An, H.**, **Gazave, E.**, **Gore, M.A.**, **Pires, J.C.**, **Robertson, L.D.** ***et al.*** (2017) Population structure and phylogenetic relationships in a diverse panel of Brassica rapa L. *Frontiers in Plant Science*, **8**, 321. Available from: https://doi.org/10.3389/fpls.2017.00321

Bradbury, P.J., **Zhang, Z.**, **Kroon, D.E.**, **Casstevens, T.M.**, **Ramdoss, Y.** & **Buckler, E.S.** (2007) TASSEL: software for association mapping of complex traits in diverse samples. *Bioinformatics*, **23**, 2633–2635. Available from: https://doi.org/10.1093/bioinformatics/btm308

Brutnell, T.P., **Bennetzen, J.L.** & **Vogel, J.P.** (2015) Brachypodium distachyon and Setaria viridis: model genetic systems for the grasses. *Annual Review of Plant Biology*, **66**, 465–485. Available from: https://doi.org/10.1146/annurev-arplant-042811-105528

Cao, H., **Xu, Y.**, **Yuan, L.**, **Bian, Y.**, **Wang, L.**, **Zhen, S.** ***et al.*** (2016) Molecular characterization of the 14-3-3 gene family in Brachypodium distachyon L. reveals high evolutionary conservation and diverse responses to abiotic stresses. *Frontiers in Plant Science*, **7**, 1099. Available from: https://doi.org/10.3389/fpls.2016.01099

Cao, J., **Jiang, M.**, **Li, P.** & **Chu, Z.** (2016) Genome-wide identification and evolutionary analyses of the PP2C gene family with their expression profiling in response to multiple stresses in Brachypodium distachyon. *BMC Genomics*, **17**, 175. Available from: https://doi.org/10.1186/s12864-016-2526-4

Catchen, J., **Hohenlohe, P.A.**, **Bassham, S.**, **Amores, A.** & **Cresko, W.A.** (2013) Stacks: an analysis tool set for population genomics. *Molecular Ecology*, **22**, 3124–3140. Available from: https://doi.org/10.1111/mec.12354

Catchen, J.M., **Amores, A.**, **Hohenlohe, P.**, **Cresko, W.** & **Postlethwait, J.H.** (2011) Stacks: building and genotyping loci de novo from short-read sequences. *G3*, **1**, 171–182. Available from: https://doi.org/10.1534/g3.111.000240

Chang, C.C., **Chow, C.C.**, **Tellier, L.C.**, **Vattikuti, S.**, **Purcell, S.M.** & **Lee, J.J.** (2015) Second-generation PLINK: rising to the challenge of larger and richer datasets. *Gigascience*, **4**, 7. Available from: https://doi.org/10.1186/s13742-015-0047-8

Chen, D., **Neumann, K.**, **Friedel, S.**, **Kilian, B.**, **Chen, M.**, **Altmann, T.** ***et al.*** (2014) Dissecting the phenotypic components of crop plant growth and drought responses based on high-throughput image analysis. *Plant Cell*, **26**, 4636–4655. Available from: https://doi.org/10.1105/tpc.114.129601

Chen, S. & **Li, H.** (2016) Heat stress regulates the expression of genes at transcriptional and post-transcriptional levels, revealed by RNA-seq in Brachypodium distachyon. *Frontiers in Plant Science*, **7**, 2067. Available from: https://doi.org/10.3389/fpls.2016.02067

Chen, Z., **Zhu, D.**, **Wu, J.**, **Cheng, Z.**, **Yan, X.**, **Deng, X.** ***et al.*** (2018) Identification of differentially accumulated proteins involved in regulating independent and combined osmosis and cadmium stress response in Brachypodium seedling roots. *Scientific Reports*, **8**, 7790. Available from: https://doi.org/10.1038/s41598-018-25959-8

Cheng, Z.-W., **Chen, Z.-Y.**, **Yan, X.**, **Bian, Y.-W.**, **Deng, X.** & **Yan, Y.-M.** (2018) Integrated physiological and proteomic analysis reveals underlying response and defense mechanisms of Brachypodium distachyon seedling leaves under osmotic stress, cadmium and their combined stresses. *Journal of Proteomics*, **170**, 1–13. Available from: https://doi.org/10.1016/j.jprot.2017.09.015

Choudhury, F.K., **Rivero, R.M.**, **Blumwald, E.** & **Mittler, R.** (2017) Reactive oxygen species, abiotic stress and stress combination. *The Plant Journal*, **90**, 856–867. Available from: https://doi.org/10.1111/tpj.13299

Chowdhury, S., **Chowdhury, A.B.**, **Kumar, M.** & **Chakraborty, S.** (2021) Revisiting regulatory roles of replication protein a in plant DNA metabolism. *Planta*, **253**, 130. Available from: https://doi.org/10.1007/s00425-021-03641-0

Claeys, H. & **Inzé, D.** (2013) The agony of choice: how plants balance growth and survival under water-limiting conditions. *Plant Physiology*, **162**, 1768–1779. Available from: https://doi.org/10.1104/pp.113.220921

Colton-Gagnon, K., **Ali-Benali, M.A.**, **Mayer, B.F.**, **Dionne, R.**, **Bertrand, A.**, **Do Carmo, S.** ***et al.*** (2014) Comparative analysis of the cold acclimation and freezing tolerance capacities of seven diploid Brachypodium distachyon accessions. *Annals of Botany*, **113**, 681–693. Available from: https://doi.org/10.1093/aob/mct283

Conway, G. (2012) *One billion hungry: Can we feed the world?*. Ithaca, NY: Cornell University Press. Available from: https://play.google.com/store/books/details?id=ZAueDgAAQBAJ

Coomey, J.H. & **Hazen, S.P.** (2015) Brachypodium distachyon as a model species to understand grass cell walls. 1–21. Available from: https://doi.org/10.1007/7397_2015_11

Corander, J., **Sirén, J.** & **Arjas, E.** (2008) Bayesian spatial modeling of genetic population structure. *Computational Statistics*, **23**, 111–129. Available from: https://doi.org/10.1007/s00180-007-0072-x

Danecek, P., **Auton, A.**, **Abecasis, G.**, **Albers, C.A.**, **Banks, E.**, **DePristo, M.A.** ***et al.*** (2011) The variant call format and VCFtools. *Bioinformatics*, **27**, 2156–2158. Available from: https://doi.org/10.1093/bioinformatics/btr330

Danecek, P., **Bonfield, J.K.**, **Liddle, J.**, **Marshall, J.**, **Ohan, V.**, **Pollard, M.O.** ***et al.*** (2021) Twelve years of SAMtools and BCFtools. *Gigascience*, **10**, 8. Available from: https://doi.org/10.1093/gigascience/giab008

Davila Olivas, N.H., **Kruijer, W.**, **Gort, G.**, **Wijnen, C.L.**, **Van Loon, J.J.A.** & **Dicke, M.** (2017) Genome-wide association analysis reveals distinct genetic architectures for single and combined stress responses in Arabidopsis thaliana. *The New Phytologist*, **213**, 838–851. Available from: https://doi.org/10.1111/nph.14165

Dell'Acqua, M., **Zuccolo, A.**, **Tuna, M.**, **Gianfranceschi, L.** & **Pè, M.E.** (2014) Targeting environmental adaptation in the monocot model Brachypodium distachyon: a multi-faceted approach. *BMC Genomics*, **15**, 801. Available from: https://doi.org/10.1186/1471-2164-15-801

Des Marais, D.L., **Lasky, J.R.**, **Verslues, P.E.**, **Chang, T.Z.** & **Juenger, T.E.** (2017) Interactive effects of water limitation and elevated temperature on the physiology, development and fitness of diverse accessions of Brachypodium distachyon. *The New Phytologist*, **214**, 132–144. Available from: https://doi.org/10.1111/nph.14316

Dokladny, K., **Zuhl, M.N.**, **Mandell, M.**, **Bhattacharya, D.**, **Schneider, S.**, **Deretic, V.** ***et al.*** (2013) Regulatory coordination between two major

intracellular homeostatic systems: heat shock response and autophagy. *The Journal of Biological Chemistry*, **288**, 14959–14972. Available from: https://doi.org/10.1074/jbc.M113.462408

Dowle, M. & **Srinivasan, A.** (2020) Data.Table: extension of 'data.Frame'. Available from: https://CRAN.R-project.org/package=data.table

Draper, J., **Mur, L.A.**, **Jenkins, G.**, **Ghosh-Biswas, G.C.**, **Bablak, P.**, **Hasterok, R.** ***et al.*** (2001) Brachypodium distachyon. A new model system for functional genomics in grasses. *Plant Physiology*, **127**, 1539–1555. Available from: https://www.ncbi.nlm.nih.gov/pubmed/11743099

Enders, T.A., **St. Dennis, S.**, **Oakland, J.**, **Callen, S.T.**, **Gehan, M.A.**, **Miller, N.D.** ***et al.*** (2019) Classifying cold-stress responses of inbred maize seedlings using RGB imaging. *Plant*, **3**, 104. Available from: https://doi.org/10.1002/pld3.104

Fahlgren, N., **Feldman, M.**, **Gehan, M.A.**, **Wilson, M.S.**, **Shyu, C.**, **Bryant, D.W.** ***et al.*** (2015) A versatile phenotyping system and analytics platform reveals diverse temporal responses to water availability in Setaria. *Molecular Plant*, **8**, 1520–1535. Available from: https://doi.org/10.1016/j.molp.2015.06.005

Fahlgren, N., **Schuhl, H.**, **Gehan, M.** ***et al.*** (2020) Danforthcenter/plantcv: PlantCV v3.8.0. Available from: https://zenodo.org/record/3700183

Faik, A., **Abouzouhair, J.** & **Sarhan, F.** (2006) Putative fasciclin-like arabinogalactan-proteins (FLA) in wheat (Triticum aestivum) and rice (Oryza sativa): identification and bioinformatic analyses. *Molecular Genetics and Genomics*, **276**, 478–494. Available from: https://doi.org/10.1007/s00438-006-0159-z

FAO, IFAD, UNICEF and WHO(2020) *The State of Food Security and Nutrition in the World 2020. Transforming food systems for affordable healthy diets*. Rome: FAO, IFAD, UNICEF, WFP and WHO.

Farooq, M., **Bramley, H.**, **Palta, J.A.** & **Siddique, K.H.M.** (2011) Heat stress in wheat during reproductive and grain-filling phases. *CRC Critical Reviews in Plant Sciences*, **30**, 491–507. Available from: https://doi.org/10.1080/07352689.2011.615687

Fick, S.E. & **Hijmans, R.J.** (2017) WorldClim 2: new 1km spatial resolution climate surfaces for global land areas. *International Journal of Climatology*, **37**, 4302–4315. Available from: https://www.worldclim.org/data/worldclim21.html

Filiz, E., **Ozdemir, B.S.**, **Budak, F.**, **Vogel, J.P.**, **Tuna, M.** & **Budak, H.** (2009) Molecular, morphological, and cytological analysis of diverse Brachypodium distachyon inbred lines. *Genome*, **52**, 876–890. Available from: https://doi.org/10.1139/g09-062

Gagné-Bourque, F., **Mayer, B.F.**, **Charron, J.-B.**, **Vali, H.**, **Bertrand, A.** & **Jabaji, S.** (2015) Accelerated growth rate and increased drought stress resilience of the model grass Brachypodium distachyon colonized by Bacillus subtilis B26. *PLoS One*, **10**, e0130456. Available from: https://doi.org/10.1371/journal.pone.0130456

Gaitanos, T.N., **Santamaria, A.**, **Jeyaprakash, A.A.**, **Wang, B.**, **Conti, E.** & **Nigg, E.A.** (2009) Stable kinetochore-microtubule interactions depend on the Ska complex and its new component Ska3/C13Orf3. *The EMBO Journal*, **28**, 1442–1452. Available from: https://doi.org/10.1038/emboj.2009.96

Gao, L., **Lee, J.S.**, **Hübner, S.**, **Hulke, B.S.**, **Qu, Y.** & **Rieseberg, L.H.** (2019) Genetic and phenotypic analyses indicate that resistance to flooding stress is uncoupled from performance in cultivated sunflower. *The New Phytologist*, **223**, 1657–1670. Available from: https://doi.org/10.1111/nph.15894

Garvin, D.F., **Gu, Y.-Q.**, **Hasterok, R.**, **Hazen, S.P.**, **Jenkins, G.**, **Mockler, T.C.** ***et al.*** (2008) Development of genetic and genomic research resources for, a new model system for grass crop research. *Crop Science*, **48**, S–69. Available from: https://www.crops.org/publications/cs/abstracts/48/Supplement_1/S-69

Gautam, T., **Saripalli, G.**, **Gahlaut, V.**, **Kumar, A.**, **Sharma, P.K.**, **Balyan, H.S.** ***et al.*** (2019) Further studies on sugar transporter (SWEET) genes in wheat (Triticum aestivum L.). *Molecular Biology Reports*, **46**, 2327–2353. Available from: https://doi.org/10.1007/s11033-019-04691-0

Gehan, M.A., **Fahlgren, N.**, **Abbasi, A.**, **Berry, J.C.**, **Callen, S.T.**, **Chavez, L.** ***et al.*** (2017) PlantCV v2: image analysis software for high-throughput plant phenotyping. *PeerJ*, **5**, e4088. Available from: https://doi.org/10.7717/peerj.4088

Gomez, L.D., **Bristow, J.K.**, **Statham, E.R.** & **McQueen-Mason, S.J.** (2008) Analysis of saccharification in Brachypodium distachyon stems under mild conditions of hydrolysis. *Biotechnology for Biofuels*, **1**, 1–12. Available from: https://doi.org/10.1186/1754-6834-1-15

Goodstein, D.M., **Shu, S.**, **Howson, R.**, **Neupane, R.**, **Hayes, R.D.**, **Fazo, J.** ***et al.*** (2012) Phytozome: a comparative platform for green plant genomics. *Nucleic Acids*, **40**, D1178–D1186. Available from: https://phytozome-next.jgi.doe.gov/i

Granier, C., **Aguirrezabal, L.**, **Chenu, K.**, **Cookson, S.J.**, **Dauzat, M.**, **Hamard, P.** ***et al.*** (2006) PHENOPSIS, an automated platform for reproducible phenotyping of plant responses to soil water deficit in Arabidopsis thaliana permitted the identification of an accession with low sensitivity to soil water deficit. *The New Phytologist*, **169**, 623–635. Available from: https://doi.org/10.1111/j.1469-8137.2005.01609.x

Gupta, A.K. & **Kaur, N.** (2005) Sugar signalling and gene expression in relation to carbohydrate metabolism under abiotic stresses in plants. *Journal of Biosciences*, **30**, 761–776. Available from: https://doi.org/10.1007/BF02703574

Gupta, P.K., **Kulwal, P.L.** & **Jaiswal, V.** (2014) Association mapping in crop plants: opportunities and challenges. *Advances in Genetics*, **85**, 109–147. Available from: https://doi.org/10.1016/B978-0-12-800271-1.00002-0

Gupta, P.K., **Kulwal, P.L.** & **Jaiswal, V.** (2019) Association mapping in plants in the post-GWAS genomics era. *Advances in Genetics*, **104**, 75–154. Available from: https://doi.org/10.1016/bs.adgen.2018.12.001

Gur, A., **Tzuri, G.**, **Meir, A.**, **Sa'ar, U.**, **Portnoy, V.**, **Katzir, N.** ***et al.*** (2017) Genome-wide linkage-disequilibrium mapping to the candidate gene level in melon (Cucumis melo). *Scientific Reports*, **7**, 9770. Available from: https://doi.org/10.1038/s41598-017-09987-4

Haas, B.J., **Delcher, A.L.**, **Mount, S.M.**, **Wortman, J.R.**, **Smith, R.K., Jr.**, **Hannick, L.I.** ***et al.*** (2003) Improving the Arabidopsis genome annotation using maximal transcript alignment assemblies. *Nucleic Acids Research*, **31**, 5654–5666. Available from: https://doi.org/10.1093/nar/gkg770

Hanisch, A., **Silljé, H.H.W.** & **Nigg, E.A.** (2006) Timely anaphase onset requires a novel spindle and kinetochore complex comprising Ska1 and Ska2. *The EMBO Journal*, **25**, 5504–5515. Available from: https://doi.org/10.1038/sj.emboj.7601426

Hedhly, A., **Nestorova, A.**, **Herrmann, A.** & **Grossniklaus, U.** (2020) Acute heat stress during stamen development affects both the germline and sporophytic lineages in Arabidopsis thaliana (L.) Heynh. *Environmental and Experimental Botany*, **173**, 103992. Available from: https://www.sciencedirect.com/science/article/pii/S0098847220300186

Helgeson, L.A., **Zelter, A.**, **Riffle, M.**, **MacCoss, M.J.**, **Asbury, C.L.** & **Davis, T.N.** (2018) Human Ska complex and Ndc80 complex interact to form a load-bearing assembly that strengthens kinetochore-microtubule attachments. *Proceedings of the National Academy of Sciences of the United States of America*, **115**, 2740–2745. Available from: https://doi.org/10.1073/pnas.1718553115

Hijmans, R.J. (2020) Raster: geographic data analysis and modeling. Available from: https://CRAN.R-project.org/package=raster

Holsinger, K.E. & **Weir, B.S.** (2009) Genetics in geographically structured populations: defining, estimating and interpreting F(ST). *Nature Reviews. Genetics*, **10**, 639–650. Available from: https://doi.org/10.1038/nrg2611

Honsdorf, N., **March, T.J.**, **Berger, B.**, **Tester, M.** & **Pillen, K.** (2014) High-throughput phenotyping to detect drought tolerance QTL in wild barley introgression lines. *PLoS One*, **9**, e97047. Available from: https://doi.org/10.1371/journal.pone.0097047

Huang, P., **Feldman, M.**, **Schroder, S.**, **Bahri, B.A.**, **Diao, X.**, **Zhi, H.** ***et al.*** (2014) Population genetics of Setaria viridis, a new model system. *Molecular Ecology*, **23**, 4912–4925. Available from: https://doi.org/10.1111/mec.12907

Ingvarsson, P.K. & **Street, N.R.** (2011) Association genetics of complex traits in plants. *The New Phytologist*, **189**, 909–922. Available from: https://doi.org/10.1111/j.1469-8137.2010.03593.x

International Brachypodium Initiative. (2010) Genome sequencing and analysis of the model grass Brachypodium distachyon. *Nature*, **463**, 763–768. Available from: https://doi.org/10.1038/nature08747

IPCC. (2014) In: Field, C.B., Barros, V.R., Dokken, D.J., Mach, K.J., Mastrandrea, M.D., Bilir, T.E. et al. (Eds.) *Climate Change 2014: Impacts, Adaptation, and Vulnerability. Part A: Global and Sectoral Aspects. Contribution of Working Group II to the Fifth Assessment Report of the Intergovernmental Panel on Climate Change*. Cambridge, United Kingdom and New York, NY, USA: Cambridge University Press.

IPCC. (2019) In: Calvo Buendia, E., Tanabe, K., Kranjc, A., Baasansuren, J., Fukuda, M., Ngarize, S. et al. (Eds.) *2019 Refinement to the 2006 IPCC*

Guidelines for National Greenhouse Gas Inventories. Switzerland: IPCC. Available from: https://www.ipcc-nggip.iges.or.jp/public/2019rf/pdf/1_Volume1/19R_V1_Ch01_Introduction.pdf

Ishibashi, T., **Koga, A.**, **Yamamoto, T.**, **Uchiyama, Y.**, **Mori, Y.**, **Hashimoto, J.** ***et al.*** (2005) Two types of replication protein a in seed plants. *The FEBS Journal*, **272**, 3270–3281. Available from: https://doi.org/10.1111/j.1742-4658.2005.04719.x

Jiang, Y., **Wang, X.**, **Yu, X.**, **Zhao, X.**, **Luo, N.**, **Pei, Z.** ***et al.*** (2017) Quantitative trait loci associated with drought tolerance in Brachypodium distachyon. *Frontiers in Plant Science*, **8**, 811. Available from: https://doi.org/10.3389/fpls.2017.00811

kapitzas. (2020) *WorldClimTiles*. Available from: https://github.com/kapitzas/WorldClimTiles

Kassambara, A. & **Mundt, F.** (2020) Factoextra: extract and visualize the results of multivariate data analyses. Available from: https://CRAN.R-project.org/package=factoextra

Kaur, H., **Manna, M.**, **Thakur, T.**, **Gautam, V.** & **Salvi, P.** (2021) Imperative role of sugar signaling and transport during drought stress responses in plants. *Physiologia Plantarum*, **171**, 833–848. Available from: https://doi.org/10.1111/ppl.13364

Kellogg, E.A. (2015) Brachypodium distachyon as a genetic model system. *Annual Review of Genetics*, **49**, 1–20. Available from: https://doi.org/10.1146/annurev-genet-112414-055135

Lê, S., **Josse, J.** & **Husson, F.** (2008) FactoMineR: a package for multivariate analysis. *Journal of Statistical Software*, **25**, 1–18. Available from: https://doi.org/10.18637/jss.v025.i01

Lee, S.J. (2016) Uncovering the genetic basis for biofuel-related traits in Brachypodium Distachyon. University of Massachusetts Amherst. Available from: https://scholarworks.umass.edu/dissertations_2/775/

Legnaioli, T., **Cuevas, J.** & **Mas, P.** (2009) TOC1 functions as a molecular switch connecting the circadian clock with plant responses to drought. *The EMBO Journal*, **28**, 3745–3757. Available from: https://doi.org/10.1038/emboj.2009.297

Leister, D., **Varotto, C.**, **Pesaresi, P.**, **Niwergall, A.** & **Salamini, F.** (1999) Large-scale evaluation of plant growth in Arabidopsis thaliana by non-invasive image analysis. *Plant Physiology and Biochemistry*, **37**, 671–678. Available from: https://www.sciencedirect.com/science/article/pii/S0981942800800972

Li, H. (2013) Aligning sequence reads, clone sequences and assembly contigs with BWA-MEM. *arXiv [q-bio.GN]* Available from: http://arxiv.org/abs/1303.3997

Liu, X. & **Chu, Z.** (2015) Genome-wide evolutionary characterization and analysis of bZIP transcription factors and their expression profiles in response to multiple abiotic stresses in Brachypodium distachyon. *BMC Genomics*, **16**, 227. Available from: https://doi.org/10.1186/s12864-015-1457-9

Liu, X., **Huang, M.**, **Fan, B.**, **Buckler, E.S.** & **Zhang, Z.** (2016) Iterative usage of fixed and random effect models for powerful and efficient genome-wide association studies. *PLoS Genetics*, **12**, e1005767. Available from: https://doi.org/10.1371/journal.pgen.1005767

Luo, N., **Liu, J.**, **Yu, X.** & **Jiang, Y.** (2011) Natural variation of drought response in Brachypodium distachyon. *Physiologia Plantarum*, **141**, 19–29. Available from: https://doi.org/10.1111/j.1399-3054.2010.01413.x

Ma, H. & **Zhao, J.** (2010) Genome-wide identification, classification, and expression analysis of the arabinogalactan protein gene family in rice (Oryza sativa L.). *Journal of Experimental Botany*, **61**, 2647–2668. Available from: https://doi.org/10.1093/jxb/erq104

MacMillan, C.P., **Mansfield, S.D.**, **Stachurski, Z.H.**, **Evans, R.** & **Southerton, S.G.** (2010) Fasciclin-like arabinogalactan proteins: specialization for stem biomechanics and cell wall architecture in Arabidopsis and eucalyptus. *The Plant Journal*, **62**, 689–703. Available from: https://doi.org/10.1111/j.1365-313X.2010.04181.x

Mickelbart, M.V., **Hasegawa, P.M.** & **Bailey-Serres, J.** (2015) Genetic mechanisms of abiotic stress tolerance that translate to crop yield stability. *Nature Reviews. Genetics*, **16**, 237–251. Available from: https://doi.org/10.1038/nrg3901

Mitchell-Olds, T., **Willis, J.H.** & **Goldstein, D.B.** (2007) Which evolutionary processes influence natural genetic variation for phenotypic traits? *Nature Reviews. Genetics*, **8**, 845–856. Available from: https://doi.org/10.1038/nrg2207

Mittler, R. (2006) Abiotic stress, the field environment and stress combination. *Trends in Plant Science*, **11**, 15–19. Available from: https://doi.org/10.1016/j.tplants.2005.11.002

Mittler, R. & **Blumwald, E.** (2010) Genetic engineering for modern agriculture: challenges and perspectives. *Annual Review of Plant Biology*, **61**, 443–462. Available from: https://doi.org/10.1146/annurev-arplant-042809-112116

Mur, L.A.J., **Allainguillaume, J.**, **Catalán, P.**, **Hasterok, R.**, **Jenkins, G.**, **Lesniewska, K.** ***et al.*** (2011) Exploiting the Brachypodium tool box in cereal and grass research. *The New Phytologist*, **191**, 334–347. Available from: https://doi.org/10.1111/j.1469-8137.2011.03748.x

Nisa, M.-U., **Huang, Y.**, **Benhamed, M.** & **Raynaud, C.** (2019) The plant DNA damage response: signaling pathways leading to growth inhibition and putative role in response to stress conditions. *Frontiers in Plant Science*, **10**, 653. Available from: https://doi.org/10.3389/fpls.2019.00653/full

Peel, F. & **Mahon, M.** (2007) Updated world map of the Koppen-Geiger climate classification. *Hydrology and Earth System Sciences*, **11**, 1633–1644. Available from: https://hess.copernicus.org/articles/11/1633/2007/hess-11-1633-2007.pdf

Pinski, A., **Betekhtin, A.**, **Sala, K.**, **Godel-Jedrychowska, K.**, **Kurczynska, E.** & **Hasterok, R.** (2019) Hydroxyproline-rich glycoproteins as markers of temperature stress in the leaves of Brachypodium distachyon. *International Journal of Molecular Sciences*, **20**, 2571. Available from: https://doi.org/10.3390/ijms20102571

Purcell, S., **Neale, B.**, **Todd-Brown, K.**, **Thomas, L.**, **Ferreira, M.A.R.**, **Bender, D.** ***et al.*** (2007) PLINK: a tool set for whole-genome association and population-based linkage analyses. *American Journal of Human Genetics*, **81**, 559–575. Available from: https://doi.org/10.1086/519795

R Core Team. (2020) *R: A language and environment for statistical computing*. Vienna, Austria: R Foundation for Statistical Computing. Available from: https://www.R-project.org/

Rajendran, K., **Tester, M.** & **Roy, S.J.** (2009) Quantifying the three main components of salinity tolerance in cereals. *Plant, Cell & Environment*, **32**, 237–249. Available from: https://doi.org/10.1111/j.1365-3040.2008.01916.x

Rasmussen, S., **Barah, P.**, **Suarez-Rodriguez, M.C.**, **Bressendorff, S.**, **Friis, P.**, **Costantino, P.** ***et al.*** (2013) Transcriptome responses to combinations of stresses in Arabidopsis. *Plant Physiology*, **161**, 1783–1794. Available from: https://doi.org/10.1104/pp.112.210773

Rivera-Contreras, I.K., **Zamora-Hernández, T.**, **Huerta-Heredia, A.A.**, **Capataz-Tafur, J.**, **Barrera-Figueroa, B.E.**, **Juntawong, P.** ***et al.*** (2016) Transcriptomic analysis of submergence-tolerant and sensitive *Brachypodium distachyon* ecotypes reveals oxidative stress as a major tolerance factor. *Scientific Reports*, **6**, 27686. Available from: https://doi.org/10.1038/srep27686

Rizhsky, L., **Liang, H.** & **Mittler, R.** (2002) The combined effect of drought stress and heat shock on gene expression in tobacco. *Plant Physiology*, **130**, 1143–1151. Available from: https://doi.org/10.1104/pp.006858

Rizhsky, L., **Liang, H.**, **Shuman, J.**, **Shulaev, V.**, **Davletova, S.** & **Mittler, R.** (2004) When defense pathways collide. The response of Arabidopsis to a combination of drought and heat stress. *Plant Physiology*, **134**, 1683–1696. Available from: https://doi.org/10.1104/pp.103.033431

Roy, R.N., **Finck, A.**, **Blair, G.J.** & **Tandon, H.L.S.** (2006) Plant nutrition for food security: a guide for integrated nutrient management, Food and Agriculture Organization of the United Nations. Available from: http://www.fao.org/fileadmin/templates/soilbiodiversity/Downloadable_files/fpnb16.pdf

Saddhe, A.A., **Manuka, R.** & **Penna, S.** (2021) Plant sugars: homeostasis and transport under abiotic stress in plants. *Physiologia Plantarum*, **171**, 739–755. Available from: https://doi.org/10.1111/ppl.13283

Salamov, A.A. & **Solovyev, V.V.** (2000) Ab initio gene finding in drosophila genomic DNA. *Genome Research*, **10**, 516–522. Available from: https://doi.org/10.1101/gr.10.4.516

Samakovli, D., **Tichá, T.**, **Vavrdová, T.**, **Ovečka, M.**, **Luptovčiak, I.**, **Zapletalová, V.** ***et al.*** (2020) YODA-HSP90 module regulates phosphorylation-dependent inactivation of SPEECHLESS to control stomatal development under acute heat stress in Arabidopsis. *Molecular Plant*, **13**, 612–633. Available from: https://doi.org/10.1016/j.molp.2020.01.001

Seifert, G.J. (2018) Fascinating fasciclins: a surprisingly widespread family of proteins that mediate interactions between the cell exterior and the

cell surface. *International Journal of Molecular Sciences*, **19**, 1628. Available from: https://doi.org/10.3390/ijms19061628

Shaar-Moshe, L., **Blumwald, E.** & **Peleg, Z.** (2017) Unique physiological and transcriptional shifts under combinations of salinity, drought, and heat. *Plant Physiology*, **174**, 421–434. Available from: https://doi.org/10.1104/pp.17.00030

Shaar-Moshe, L., **Hayouka, R.**, **Roessner, U.** & **Peleg, Z.** (2019) Phenotypic and metabolic plasticity shapes life-history strategies under combinations of abiotic stresses. *Plant Direct*, **3**, e00113. Available from: https://doi.org/10.1002/pld3.113

Shi, H., **Ye, T.**, **Song, B.**, **Qi, X.** & **Chan, Z.** (2015) Comparative physiological and metabolomic responses of four Brachypodium distachyon varieties contrasting in drought stress resistance. *Acta Physiologiae Plantarum*, **37**, 122. Available from: https://doi.org/10.1007/s11738-015-1873-0

Skirycz, A., **Vandenbroucke, K.**, **Clauw, P.**, **Maleux, K.**, **de Meyer, B.**, **Dhondt, S.** ***et al.*** (2011) Survival and growth of Arabidopsis plants given limited water are not equal. *Nature Biotechnology*, **29**, 212–214. Available from: https://doi.org/10.1038/nbt.1800

Smit, A.F.A., **Hubley, R.** & **Green, P.** (1996-2010) *RepeatMasker Open-3.0*. Available from: http://www.repeatmasker.org

Sun, Y., **Geng, Q.**, **Du, Y.**, **Yang, X.** & **Zhai, H.** (2017) Induction of cyclic electron flow around photosystem I during heat stress in grape leaves. *Plant Science*, **256**, 65–71. Available from: https://doi.org/10.1016/j.plantsci.2016.12.004

Sun, Y., **Liu, F.**, **Bendevis, M.**, **Shabala, S.** & **Jacobsen, S.-E.** (2014) Sensitivity of two quinoa (chenopodiumquinoa Willd.) varieties to progressive drought stress. *Journal of Agronomy and Crop Science*, **200**, 12–23. Available from: https://doi.org/10.1111/jac.12042

Suzuki, N., **Bassil, E.**, **Hamilton, J.S.**, **Inupakutika, M.A.**, **Zandalinas, S.I.**, **Tripathy, D.** ***et al.*** (2016) ABA is required for plant acclimation to a combination of salt and heat stress. *PLoS One*, **11**, e0147625. Available from: https://doi.org/10.1371/journal.pone.0147625

Swaminathan, M.S. (2012) Combating hunger. *Science*, **338**, 1009. Available from: https://doi.org/10.1126/science.1231305

Tyler, L., **Lee, S.J.**, **Young, N.D.**, **Delulio, G.A.**, **Benavente, E.**, **Reagon, M.** ***et al.*** (2016) Population structure in the model grass is highly correlated with flowering differences across broad geographic areas. *Plant Genome*, **9**, 74. Available from: https://doi.org/10.3835/plantgenome2015.08.0074

United Nations. (2019) World population Prospects 2019: Highlights, UN. Popul. Newsl.

VanRaden, P.M. (2008) Efficient methods to compute genomic predictions. *Journal of Dairy Science*, **91**, 4414–4423. Available from: https://doi.org/10.3168/jds.2007-0980

Vogel, J.P., **Tuna, M.**, **Budak, H.**, **Huo, N.**, **Gu, Y.Q.** & **Steinwand, M.A.** (2009) Development of SSR markers and analysis of diversity in Turkish populations of Brachypodium distachyon. *BMC Plant Biology*, **9**, 88. Available from: https://doi.org/10.1186/1471-2229-9-88

Wang, J. & **Zhang, Z.** (2021) GAPIT version 3: boosting power and accuracy for genomic association and prediction. *Genomics, Proteomics & Bioinformatics*, **19**, 629–640. Available from: https://doi.org/10.1016/j.gpb.2021.08.005

Warnes, G.R., **Bolker, B.**, **Bonebakker, L.** ***et al.*** (2020) gplots: various R programming tools for plotting data. Available from: https://CRAN.R-project.org/package=gplots

Wei, T. & **Simko, V.** (2017) R package "corrplot": visualization of a correlation matrix. Available from: https://github.com/taiyun/corrplot

Weir, B.S. & **Cockerham, C.C.** (1984) Estimating F-statistics for the analysis of population structure. *Evolution*, **38**, 1358–1370. Available from: https://doi.org/10.1111/j.1558-5646.1984.tb05657.x

Wickham, H. (2007) Reshaping data with the reshape package. *Journal of Statistical Software*, **21**, 1–20. Available from: http://www.jstatsoft.org/v21/i12/

Wickham, H. (2011) The split-apply-combine strategy for data analysis. *Journal of Statistical Software*, **40**, 1–29. Available from: http://www.jstatsoft.org/v40/i01/

Wickham, H. (2016) *ggplot2: elegant graphics for data analysis*. New York: Springer-Verlag.

Wickham, H. (2020) tidyr: Tidy Messy Data. Available from: https://CRAN.R-project.org/package=tidyr

Wickham, H., **François, R.**, **Henry, L.** and **Müller, K.** (2021) Dplyr: a grammar of data manipulation. Available from: https://CRAN.R-project.org/package=dplyr.

Wickham, H., **Hester, J.** and **Bryan, J.** (2022) Readr: read rectangular text data. Available from: https://readr.tidyverse.org, https://github.com/tidyverse/readr

Wilson, P., **Streich, J.** & **Borevitz, J.** (2015) Genomic diversity and climate adaptation in Brachypodium. *Genetics and genomics of Brachypodium*, **18**, 107–127. Available from: https://doi.org/10.1007/7397_2015_18

Wilson, P.B., **Streich, J.C.**, **Murray, K.D.**, **Eichten, S.R.**, **Cheng, R.**, **Aitken, N.C.** ***et al.*** (2019) Global diversity of the Brachypodium species complex as a resource for genome-wide association studies demonstrated for agronomic traits in response to climate. *Genetics*, **211**, 317–331. Available from: https://doi.org/10.1534/genetics.118.301589

Wright, S. (1965) The interpretation of population structure by F-statistics with special regard to systems of mating. *Evolution*, **19**, 395–420. Available from: http://www.jstor.org/stable/2406450

Xiao, Y., **Liu, H.**, **Wu, L.**, **Warburton, M.** & **Yan, J.** (2017) Genome-wide association studies in maize: praise and stargaze. *Molecular Plant*, **10**, 359–374. Available from: https://doi.org/10.1016/j.molp.2016.12.008

Yamada, M. & **Goshima, G.** (2017) Mitotic spindle assembly in land plants: molecules and mechanisms. *Biology*, **6**, 6. Available from: https://doi.org/10.3390/biology6010006

Yeh, R.F., **Lim, L.P.** & **Burge, C.B.** (2001) Computational inference of homologous gene structures in the human genome. *Genome Research*, **11**, 803–816. Available from: https://doi.org/10.1101/gr.175701

You, J., **Zhang, L.**, **Song, B.**, **Qi, X.** & **Chan, Z.** (2015) Systematic analysis and identification of stress-responsive genes of the NAC gene family in Brachypodium distachyon. *PLoS One*, **10**, e0122027. Available from: https://doi.org/10.1371/journal.pone.0122027

Zhang, X., **Zang, R.** & **Li, C.** (2004) Population differences in physiological and morphological adaptations of Populus davidiana seedlings in response to progressive drought stress. *Plant Science*, **166**, 791–797. Available from: https://www.sciencedirect.com/science/article/pii/S0168945203004989

Zheng, X., **Fahlgren, N.**, **Abbasi, A.**, **Berry, J.C.** & **Carrington, J.C.** (2019) Antiviral ARGONAUTEs against turnip crinkle virus revealed by image-based trait analysis. *Plant Physiology*, **180**, 1418–1435. Available from: https://doi.org/10.1104/pp.19.00121

Zhou, J., **Wang, J.**, **Yu, J.-Q.** & **Chen, Z.** (2014) Role and regulation of autophagy in heat stress responses of tomato plants. *Frontiers in Plant Science*, **5**, 174. Available from: https://doi.org/10.3389/fpls.2014.00174

Ziegler, G.R., **Hartsock, R.H.** & **Baxter, I.** (2015) Zbrowse: an interactive GWAS results browser. *PeerJ Computer Science*, **1**, e3. Available from: https://peerj.com/articles/cs-3/